Air-Sea Exchange in Hurricanes: Synthesis of Observations from the Coupled Boundary Layer Air-Sea Transfer Experiment

Peter G. Black[1*], Eric A. D'Asaro[2], William M. Drennan[3], Jeffrey R. French[4],

Pearn P. Niiler[5], Thomas B. Sanford[2], Eric J. Terrill[5], Edward J. Walsh[6] and Jun A. Zhang[3]

[1]NOAA/AOML Hurricane Research Division, Miami, Florida

[2]University of Washington, Applied Physics Laboratory, Seattle Washington

[3]University of Miami, Rosenstiel School of Marine and Atmospheric Science, Miami, Florida

[4,]University of Wyoming, Department of Atmospheric Science, Laramie, Wyoming

[5]University of California, Scripps Institution for Oceanography, La Jolla, California

[6]NASA, Goddard Space Flight Center, Wallops Island, Virginia

Re-Submitted to BAMS

July 2006

* *Corresponding author address:* Peter G. Black, NOAA/AOML Hurricane Research Division, Miami, FL 33149
E-mail peter.black@noaa.gov

Combining airborne remote, in-situ and expendable probe sensors with air-deployed ocean surface drifting and subsurface profiling platforms provides an observational strategy for expanded knowledge of illusive high wind air-sea flux observations from hurricanes imbedded in difficult-to-predict, large-scale atmospheric weather patterns.

Abstract

The CBLAST field program conducted from 2002-2004 has provided a wealth of new air-sea interaction observations in hurricanes. The wind speed range for which turbulent momentum and moisture exchange coefficients have been derived based upon direct flux measurements has been extended by 30 and 60 percent, respectively, from airborne observations in Hurricanes Fabian and Isabel in 2003. The drag coefficient (C_D) values derived from CBLAST momentum flux measurements show C_D becoming invariant with wind speed near a 23 ms^{-1} threshold rather than a hurricane-force threshold near 33 ms^{-1}. Values above 23 ms^{-1} are lower than previous open ocean measurements.

The Dalton number estimates (C_E) derived from CBLAST moisture flux measurements are shown to be invariant with wind speed to 30 ms^{-1}, in approximate agreement with previous measurements at lower winds. These observations imply a C_E/C_D ratio of approximately 0.7, suggesting that additional energy sources are necessary for hurricanes to achieve their maximum potential intensity. One such additional mechanism for augmented moisture flux in the boundary layer might be linear coherent features, observed by CBLAST 2002 measurements, to have wavelengths of 0.9 to 1.2 km. Linear features of the same wavelength range were observed in nearly-concurrent RADARSAT Synthetic Aperture Radar (SAR) imagery.

As a complement to the aircraft measurement program, arrays of drifting buoys and subsurface floats were successfully deployed ahead of Hurricanes Fabian (2003) and Frances (2004): 16 (6) and 38 (14) drifters (floats) respectively in the two storms. An unprecedented set

of observations was obtained, providing a four-dimensional view of the ocean response to a hurricane for the first time ever. Two types of surface drifters and three types of floats provided observations of surface and subsurface oceanic currents, temperature, salinity, gas exchange, bubble concentrations and surface wave spectra to a depth of 200 m on a continuous basis before, during and after storm passage, as well as surface atmospheric observations of wind speed (via acoustic hydrophone) and direction, rain rate and pressure. Float observations indicated deepening of the mixed layer from 40 to 120 m in approximately 8 hr with a corresponding decrease in SST in the right-rear quadrant of 3.2ºC in 11 hr, roughly one-half inertial period. Strong inertial currents with a peak amplitude of 1.5 ms^{-1} were observed. Vertical structure showed the critical Richardson number was reached sporadically during the mixed layer deepening event, suggesting shear-induced mixing as a prominent mechanism during storm passage. Peak significant waves of 11m were observed from the floats to complement the aircraft-measured directional wave spectra.

1. Introduction

The Coupled Boundary Layer Air-Sea Transfer (CBLAST) experiment was conducted during 2000-2005 to improve our fundamental understanding of physical processes at the air-sea interface. We focus here on the CBLAST-Hurricane component, which included experimental observations of the air-sea exchange process in high winds suitable for improving hurricane track and intensity model physics. Other CBLAST activities focused on low wind dynamics (Edson et al 2006) and coupled modeling of hurricanes (Chen et al 2006).

Energy exchange at the air-sea interface is one of three major physical processes governing hurricane intensity change. The others are environmental interactions with

surrounding large-scale features in the atmosphere and internal dynamics such as eyewall replacement cycles and cloud microphysics. The air-sea exchange of heat, moisture and momentum determines how hurricanes gain their strength and intensity from the ocean. This has become an extremely important problem over the past several years as we have entered a new era of greater numbers of hurricanes (Goldenberg, 2001), as well as an era of more intense hurricanes (Emanuel, 2005; Webster et al., 2005; Landsea, 2005). The past two years have witnessed an increase in the number of major hurricane landfalls. While efforts to forecast hurricane track have improved greatly over the past 15 years, our ability to forecast hurricane intensity has shown little skill (DeMaria et al., 2005). With more hurricane threats on the U. S. and Caribbean coastlines, the effort to improve hurricane intensity forecasting has taken on greater urgency. The mitigation actions that are taken by emergency management officials, local, state and federal governments and private industry all depend on predictions of intensity thresholds at and near landfall. In response to this need for improved hurricane intensity forecasts, the Office of Naval Research (ONR) initiated the CBLAST program to complement ongoing hurricane intensity research programs in universities and government laboratories such as the Hurricane Research Division.

The resulting CBLAST Hurricane experiment became a cooperative undertaking between the ONR, NOAA's Office of Oceanic and Atmospheric Research (OAR), Hurricane Research Division (HRD), Aircraft Operations Center (AOC), including it's United States Weather Research Program (USWRP) and the United States Air Force Reserve Command's (AFRC's) 53rd Weather Reconnaissance Squadron (WRS).ONR provided support for 17 PI's (see Table 1) from universities and government laboratories. NOAA provided aircraft flight hour support for two WP-3D research aircraft, expendable probes and Hurricane Field Program

infrastructure. AFRC, through the 53rd WRS, provided infrastructure support, specialized expertise in air deployment of large platforms and WC-130J and C-130J aircraft support. The observational strategies and initial results of this effort are described in the following pages.

The overarching goal of CBLAST was to provide new physical understanding that would improve forecasting of hurricane intensity change with the new suite of operational models now undergoing testing and evaluation at the Naval Research Laboratory (NRL) and at NOAA's Environmental Modeling Center (EMC). CBLAST focused an intensive effort on observing air-sea interaction processes within hurricanes because of the recognized lack of knowledge of the physics of air-sea exchange at winds above gale force. Prior to CBLAST, no in-situ air-sea flux measurements existed at wind speeds above 22 ms^{-1}. Parameterization schemes used to approximate air-sea transfer at hurricane wind speeds were simply an extrapolation of low wind measurements with the assumption that the physical processes were the same – despite clear evidence to the contrary! A key goal of CBLAST was to extend the range of observations for exchange coefficients of momentum, heat and moisture across the air-sea interface to hurricane force winds, and above.

2. CBLAST CONCEPT AND OBSERVATION PLAN

The CBLAST experimental design consisted of two major observational components: 1) airborne in-situ and remote sensing instrumentation flown into hurricanes by the two NOAA WP-3D aircraft and 2) air-deployed surface drifting buoys and subsurface profiling floats. This was intended to provide a mix of 'snapshots' of inner-core hurricane conditions each day over a 2-4 day period together with a continuous time series of events at particular ocean locations. A third component, available based on operational needs, consisted of the hurricane synoptic

surveillance program designed for improved track forecasting. It provided, on occasion, concurrent high-level NOAA G-IV jet aircraft flights in the hurricane environment, deploying GPS dropsondes to profile the steering currents and significant synoptic features, in addition to reconnaissance flights within the hurricane's inner core from the WC-130H aircraft, operated by AFRC 53rd WRS. Polar-orbiting and geostationary satellite platforms provided additional remote sensing measurements in the hurricane's inner core and environment. This approach provided an overarching data base to allow intensity changes from air-sea interaction causes to be separable from those due to atmospheric environmental interactions and internal dynamics.

The aircraft component of CBLAST had two modules: a) an aircraft stepped descent module and b) an inner-core survey module. The former was designed to focus on in-situ air-sea flux and spray measurements, while the latter was to focus on large-scale structure, eyewall flux budget measurements and documentation of internal dynamics. The centerpiece of this effort involved a multi-sonde sequence of 8-12 GPS dropsondes dropped from coordinated WP-3Ds flying in tandem at different altitudes across the hurricane eyewall and eye. See Fig. 1 for a schematic of a typical flight plan. Each module consisted of several options related to precise experimental patterns dictated by prevailing conditions and available time on station. For instance, the stepped descents (Fig. 2), designed to probe the hurricane boundary layer down to as low as 70m above the sea, were only carried out in clear air conditions between rainbands.

Both modules were complemented with an array of airborne remote and in-situ sensors. Air-deployed drifting buoys (drifters) and oceanographic floats (auto-profiling oceanographic radiosondes) were designed to further complement the airborne in-situ and remote sensing of the air-sea interface. This drifter/float air-deployment module consisted of arrays of sensors measuring continuous time series of surface and upper ocean conditions before, during and after

hurricane passage. Together the aircraft and drifter/float array provided a unique description of air-sea fluxes, surface wave and upper ocean conditions in hurricane conditions never before achieved. In a similar fashion, the inner core survey module provided observations of significant changes in the inner core dynamics occurring concurrently with observed air-sea processes.

3. CASE STUDIES

The CBLAST experimental effort began in 2000 with the development of seven new airborne instrument systems, three new oceanographic float designs, 2 drifting buoy designs, the flight pattern strategy and the air-deployment strategy, including the WC-130J air-deployment certification and air-drop certification of 3 platform types. The new airborne instrument systems were 1) Best Aircraft Turbulence (BAT) probe for fast response temperature and u-,v-,w-wind components, 2) a modified LICOR fast response hygrometer, 3) CIP particle spectrometer and 4) Particle Doppler Analyzer (PDA) for sea spray droplet observation, 5) Scripps downward-looking, high-speed visible and infrared video camera systems for wave breaking observations, 6) Stepped and Simultaneous Frequency Microwave Radiometers (SFMR and USFMR) for surface wind speed and 7) the Integrated Wind and Rain Atmospheric Profiler (IWRAP) for continuous boundary layer and surface wind vector profiles.

These systems were built in 2001 and flight- tested in 2002. Also deployed were three existing systems: 1) Tail (TA) Doppler radar for boundary layer wind structure, 2) Lower Fuselage (LF) weather radar for hurricane precipitation structure and 3) Scanning Radar Altimeter (SRA) for directional wave spectra. Two storms, Edouard and Isidore, were flown in 2002, the first to test the new stepped-descent flight pattern strategy and the second to test extended low level flight pattern for detection of linear coherent turbulence structures, sometimes referred to as ‘roll vortex’ or ‘secondary boundary layer’ circulations. The CBLAST

field program began in earnest in 2003 with the survey flight pattern flown on 6 days by the two NOAA WP-3D aircraft (a total of 12 flights, including 12 stepped-descent patterns) in Hurricanes Fabian and Isabel from a staging base in St. Croix, U.S. Virgin Islands. An additional 10 AFRC WC-130H reconnaissance flights and 3 NOAA G-IV surveillance flights were also flown during this period. An array of 16 drifting buoys and 6 floats were deployed by the 53rd WRS from a WC-130J aircraft ahead of Hurricane Fabian.

An engine failure due to salt build-up occurred near the end of the sixth flight which resulted in new safety regulations requiring a chemical engine wash after each flight below 340 m. CBLAST flights in 2004 continued, but were restricted to flight levels above the boundary layer. The CBLAST flights in 2004 were in Hurricanes Frances on 4 days, Ivan on 5 days and Jeanne on 3 days. The key success in 2004 was the air-deployment by the 53rd WRS of 38 drifting buoys (30 Minimet; 8 ADOS) and 14 floats (9 ARGO/SOLO; 2 Lagrangian; 3 EM/APEX) ahead of Hurricane Frances on Aug 31. All drifters and floats were deployed successfully. The floats were recovered by the UNOLS ship R/V Cape Hatteras between Sept 27 and Oct 4, approximately 4 weeks after deployment.

4. Key results from the aircraft component

a. First turbulence measurements in tropical storm and hurricane force winds

The principal results from the aircraft component of CBLAST were the estimation of surface momentum and enthalpy flux from direct eddy correlation measurements using two newly modified airborne instrument packages: the BAT Probe and the LICOR fast response hygrometer, shown mounted on the WP-3D aircraft in Fig. 3. The results are based on

measurements obtained during 15 stepped-descent patterns flown in Hurricanes Fabian and Isabel in 2003 (Fig. 4). These are the first direct flux measurements ever in a hurricane and the first in a tropical storm since the 'gust probe' measurements of Moss and Merceret (1976, 1977) and Moss (1978) in the periphery of Tropical Storm Eloise on Sept 17, 1975[1], where their estimated surface winds were ~ 20 ms^{-1}. Data from a total of 48 (42) flux runs were used to compute independent estimates of the momentum (humidity) flux. All of the flux runs were flown between 70 and 400m at an airspeed of close to 113 ms^{-1}. Measurements from GPS dropsondes indicate that the top of the hurricane planetary boundary layer (PBL), defined as the top of the constant potential temperature layer, was approximately 500 m (Drennan, et al., 2006). Leg lengths ranged from 13 to 55 km, with an average length of 28 km. Fluxes of momentum and humidity were computed using eddy correlation. Profiles of fluxes were analyzed for individual stepped descents. There was no significant height dependence of humidity flux within the PBL. Momentum flux decreased to only 50 to 75 percent of the surface values near the top of the PBL. Surface friction velocity was computed following Donelan (1990). Ten-meter neutral wind (U_{10N}) was taken from leg-averaged measurements (approximately 5 minutes) from a nadir-pointing SFMR (Uhlhorn and Black, 2003; Uhlhorn, et al., 2006). The drag coefficient (C_{D10N}, referred to hereafter as C_D) was computed directly from the friction velocity and U_{10N}. Surface saturated specific humidity, q_0, was estimated based on the sea surface temperature (SST), provided by an infrared radiometer on the aircraft, averaged along the flight track, and corrected for intervening atmospheric absorption. A linear regression line was fit to the measured SST values at each stair-step altitude and the surface value extrapolated. The difference between the

[1] While the authors refer to their measurements in 'Hurricane' Eloise, the National Hurricane Center Best Track archives (http://www.nhc.noaa.gov/tracks1851to2005_atl.txt) lists the peak surface winds for Eloise on Sept 17, 1975, when the center was over Hispañola (Hebert 1976), as tropical storm strength, i.e. 22-25 ms^{-1}, for the 18-00 UTC period of the research flight.

extrapolated surface value and the average value for each flux run was then computed and used to correct the measured SST to the true value. Additional details on this method can be found in Drennan et al. 2006. Neutral ten-meter specific humidity, q_{10N}, was estimated using a logarithmic profile to extrapolate the flight level measurements to 10 m. The moisture exchange coefficient, or Dalton number, (C_{E10N}, referred to hereafter as C_E) for each flux run was computed directly from the humidity flux, U_{10N}, q_0 and q_{10N}. Details and justification of the above discussion can be found in French et al. (2006) and Drennan et al. (2006). Of course, in an environment where individual wave heights can exceed 20m, the meaning of 10m bulk coefficients should be questioned. We consider them useful as reference values, 10m being the lowest level for many atmospheric models.

When CBLAST C_D and C_E results are compared with other studies (Figs. 5 and 6), one can see that they represent a 32 and 61 percent increase, respectively, of the wind speed range of prior observations. It is apparent that the CBLAST high-wind C_D values represent a systematic departure from prior estimates. Several surprising results emerged from these measurements. Primarily, CBLAST C_D measurements become nearly invariant with wind speed above a 23 ms^{-1} threshold (Fig. 5). This is a full 10 to 12 ms^{-1} less than the hurricane-force threshold of 33 ms^{-1} obtained using GPS dropsonde measurements by Powell et al. (2003) and laboratory tank measurements by Donelan et al. (2004).

CBLAST C_D measurements (Fig. 5) agree with previous open-ocean, gale-force wind measurements in the range 17 - 22 ms^{-1} for fully developed seas in the North Pacific at Ocean Weather Ship Papa, (Large and Pond, 1981) in the North Atlantic at Sable Island (Smith, 1980) and in the Southern Oceans from a research vessel (Yelland, et al., 1998). Values are lower than C_D observations in fetch-limited wave conditions during HEXOS in the North Sea (Smith, et al.,

1992), for COARE 3.0 conditions (Fariall et al., 2003) and for CBLAST-low (Edson et al., 2006) . Estimates of C_D show little dependence on quadrant of the storm in which the measurements were obtained. However, it should be noted that the natural variability in the data provide less than overwhelming confidence of this result. The value of C_D differs little between regions of young, growing waves in the right-rear quadrant in a swell-following environment and regions in the right-front and left-front quadrants where the local sea was older, less steep and higher, with swell at increasing crossing angles with respect to the wind of up to 90 degrees (Wright et al., 2001), a result discussed further in the following sub-section. Another new finding suggests that moisture flux measurements are relatively constant with height within the hurricane boundary layer. Finally, we find that estimates of C_E above 20 ms^{-1} are in good agreement with the results from HEXOS (DeCosmo et al. 1996; modified as per Fairall et al. 2003) and COARE 3.0 (Fairall et al. 2003) extrapolated from 19 ms^{-1} through our range of measurements (Fig. 6). This suggests that C_E is constant with wind speed to hurricane force winds of 33 ms^{-1}.

It is obvious that while CBLAST extended the wind speed range of prior C_D and C_E observations, a further increase of the wind speed range is required to validate flux estimates in hurricane-force wind conditions, where physical processes may depart significantly from tropical storm wind conditions as the importance of sea spray and other poorly understood phenomena such as 'roll-vortex' features, may increase dramatically. Budget and sea spray studies are underway to estimate CD and CE for hurricane-force conditions by Emanuel (personal communication) using the CBLAST rapid deployment eyewall dropsondes in Fabian and Isabel and by Fairall (personal communication) using laboratory measurements.

Emanuel (1986, 1995) has shown that the ratio of C_E/C_D is an important parameter in estimating hurricane potential intensity. The new C_D and C_E observations along with the new

highly-reliable SFMR surface wind measurements (Uhlhorn and Black, 2003; Uhlhorn, et al., 2006) show C_E/C_D values to average near 0.7 for tropical storm conditions, slightly below the Emanuel (1995) threshold for hurricane development of 0.75 (Fig. 7). C_E/C_D ratio estimates from budget methodology by Emanuel (personal communication) for axisymmetric mean surface winds of 50 ms^{-1} in Isabel suggest that the ratio may increase significantly above our values for intense hurricane conditions. On the other hand, Andreas and Emanuel (2001) have suggested that the role of spray may act to simultaneously increase C_D and C_E, leaving the ratio nearly equal to our values at high winds. This would require another explanation for how intense hurricanes develop and are maintained. The implications of $C_E/C_D \sim 0.7$ for intense storms have been investigated by Montgomery et al., 2006, and Bell and Montgomery (2006) which indicate that 'superintense' conditions leading to sustained CAT 4 and 5 conditions, such as observed in Isabel, are a result of strong air-sea interaction inward from the hurricane eyewall leading to augmented horizontal entropy transport via enhanced frictional inflow and eyewall mesovortices. They suggested that this mechanism was a key reason why Isabel maintained CAT 5 status for 3 days.

b. Surface wave observations

The Scanning Radar Altimeter (SRA) on one of the P3 aircraft recorded huge data sets of wave images and 2D wave spectra in all quadrants of CBLAST storms in Fabian in 2003 and throughout CBLAST storms in 2004. A wave image typical of this data set (Fig. 8) from the front quadrant of Hurricane Fabian near 500 m flight altitude illustrates the predominant 300 m swell. Superimposed on the swell is the local sea with wavelengths of about 80-100 m crossing at a 90º angle. This is typical of conditions depicted in sector III of Fig. 9, which illustrate 3 sectors of distinctly different 2D wave spectra in Hurricane Bonnie (1998), discussed by Wright

et al., 2001. The spectra in sector I tend to be tri-modal with 2 swell peaks plus the local sea. The spectra in sector II tend to transition from tri-modal to bi-modal with the swell following within 30 degrees of the local sea. The spectra in sector III tend to transition from bimodal to unimodal depending on whether the local sea is resolved. The swell tends to propagate at about a 90-degree angle to the local sea in this region.

A further illustration of the behavior of the swell relative to the local sea as a function of azimuth is shown in Fig 10, from SRA measurements throughout Hurricane Ivan (2004). Fig. 10 shows an HRD H*WIND surface wind analysis (Powell and Houston, 1996; Powell et al., 1998; Powell and Houston, 1998)- based primarily on SFMR surface wind data- for Hurricane Ivan on 14 September 2004 when Ivan was moving northwest. Twelve SRA spectra about 80 km from the eye are shown in Fig. 10. In the right-front quadrant (sector II/III boundary) the wave field is unimodal with 350 m wavelength and 11.4 m wave height. Directly to the right of the track the wavelength shortens to about 260 m and the spectrum broadens and becomes bimodal. In the right-rear quadrant the wave height decreases and the spectrum becomes trimodal. In the rear quadrant of Ivan, as was the case with Bonnie (Fig. 9), the wave height and length reach minimum values of 5.6 m and 190 m, about half their values in the right forward quadrant. This suggests the waves are young, steep and short in the right-rear quadrant and older, flatter and longer in the right front and left front quadrants. To the left-rear and left-front of the eye, the wind and waves are about at right angles to each other.

The expectation was that the exchange coefficients would exhibit a variability that depended on the characteristics of the 2D wave spectrum. This has turned out to not be the case as one can see by comparing Figs 5 and 6 with Fig. 10. What this says, and what emerges as the second major conclusion for CBLAST hurricane measurements, is that surface fluxes and

exchange coefficients derived from them (Figs. 5-6) appear not to be a function of the variation in the relationship between the long wavelength swell and the shorter wavelength local sea, at least between tropical storm and hurricane force wind radii.

c. Evidence for secondary boundary layer circulations

Strong evidence was found for the existence of 'roll vortex' secondary boundary layer circulations in hurricanes. Complementing the CBLAST flights in 2002-2004 were a number of RADARSAT and ENVISAT Synthetic Aperture Radar (SAR) passes (see Fig. 11, top) over the storms which all showed streaks in the radar backscatter with wavelengths on the order of 800-1000 m. These were most prominent in the front semicircle of the storm. Spectral analysis of these images over 5km square ocean cells were able to retrieve a direction that was nearly equal to the wind direction, as well as a mean wavelength (Katsaros et al., 2002). Fig. 11 (bottom) illustrates a histogram averaged over six such 2D spectra (6 km square) that shows a peak near 900 m. This value is close to that determined from ground-based WSR-88D Doppler radar observations in landfalling hurricanes (Morrison et al., 2005). Their results are supported by more recent higher-resolution portable Doppler radar observations in landfalling hurricanes (Losorlo et al., 2006a, b) and by Doppler on Wheels (DOW) high resolution portable Doppler radar observations in Hurricane Fran (Wurman and Winslow, 1998), and more recently in Hurricane Rita (Wurman et al., 2006). With these studies, the range of wavelengths of these linear features are well documented over land in landfalling hurricanes. Now, RADARSAT and ENVISAT SAR observations suggest they are also endemic to the hurricane wind field over the ocean.

To further emphasize possible boundary layer manifestation of these linear features, the along-wind component of the velocity co-spectrum was computed from gust probe data in

Hurricane Isidore (2002) along a 75 km leg flown at 300 m, near the middle of the hurricane planetary boundary layer with a depth of 500 m (deduced from the depth of constant potential temperature layers measured by dropsondes). The first part of the leg was in the radial direction toward the eye and showed a significant peak in the co-spectrum near 900 m (Fig. 12), in close agreement with the scales from the SAR histogram (Fig. 11, bottom). This peak disappeared when the aircraft turned and flew along wind. The significance of these observations are that these linear features, and their possible major effects on air-sea fluxes as suggested by Morrison et al. (2005) and Foster (2005), are not currently modeled in any major hurricane coupled modeling effort, and may be an important factor in predictions of hurricane intensity change. This leads to the third major CBLAST finding to date, i.e. that secondary boundary layer circulations, while not a major thrust of the original CBLAST plan, are a significant factor in the hurricane boundary layer flow field and are a likewise significant factor in air-sea fluxes.

5. Key Results from the Air-Deployed Oceanographic Sensor Component of CBLAST Hurricane

The 54 buoys and floats deployed into Hurricane Frances in 2004 yielded a wealth of information on ocean structure and structure changes induced by the hurricane within and below the ocean mixed layer: the first ever 4D ocean structure observations beneath a hurricane. Detailed measurements of the ocean and air-sea interface beneath hurricanes were made using several varieties of autonomous floats and drifters that were air-deployed ahead of the storm. The technology for these devices has matured rapidly in recent years so that they are now deployed in large numbers as part of the developing system for the Integrated Ocean Observing System (IOOS). For CBLAST, air-deployment systems were developed for existing platforms and they were equipped with new sensors to measure properties of the air-sea interface. The goal of these

investigations was to understand the properties of the air-sea interface and upper ocean at wind speeds greater than 30 ms^{-1}, to determine the associated air-sea fluxes and the effect of these on hurricane intensification.

The region of high winds beneath a hurricane is quite small: a few hundred km in diameter for the largest storms, much less for a typical storm. Accordingly, the probability of measuring high winds from an array of instruments prepositioned in "hurricane alley" is small. As with meteorological studies of hurricanes, a viable sampling plan must rely on real-time measurements of storm position, reliable forecasts of future storm tracks and the ability of aircraft to deploy sensors in or near an active storm based on this information. Accordingly, close cooperation was essential between the National Hurricane Center, which supplied the storm forecasts, the scientific team, who adapted the sampling array to these changing conditions, and the 53rd Air Force Reserve squadron, who deployed the instruments. Equally important was the use of UNOLS ships to recover the floats after the hurricane had passed.

The five varieties of oceanographic instruments used in CBLAST Hurricane can be divided into two categories: *drifters* and *floats*. Details of each instrument type are shown in Table 3. Fig. 13 shows drawings of each instrument and a schematic of their operation in Hurricane Frances (2004).

Drifters aim to follow the ocean current at 15m depth while measuring both near-surface atmospheric and upper-ocean properties. A small surface float supports a much larger drogue centered at 15m depth. The large drogue causes the drifter to nearly follow the horizontal water motion at approximately 15m. A transmitter in the surface drifter sends data to the ARGOS satellite system. The same signals are used to track the drifter. The standard drifter measurements

are position and near-surface temperature. The CBLAST drifters carried additional sensors. Minimet drifters are also designed to estimate wind speed using the sound level at 8 kHz (Nystuen and Selsor, 1997) and wind direction using a vane on the surface float. Evaluation of the accuracy of this approach at hurricane wind speeds is still under way. ADOS drifters additionally measure the temperature profile to 100m depth.

The three varieties of floats are shown in Fig. 13. All floats operate by mechanically changing their volume, and thus their density, in order to control their depth. By making themselves light, they can profile to the surface thereby extending an antenna out of the water enabling them to obtain a GPS fix and relay data to and receive instructions from their shore-based operators. The EM-APEX floats (Fig 13, green lines) operated as profilers, continuously cycling while measuring temperature, salinity and velocity. Profiles extended from the surface to 200m with profiles to 500m every half inertial period. During the storm, the top of the profiles terminated at 50m. The Lagrangian floats (D'Asaro, 2003), profiled only before and after the storm (Fig. 13 black line). During the storm, they remained neutrally buoyant, following the three-dimensional motion of water parcels in the highly turbulent upper boundary layer. They measured temperature, salinity and gas concentration. The SOLO floats combined profiling of temperature, salinity and oxygen from the surface to approximately 200m (Fig. 13, blue line) while hovering at about 40m for a period of time during each dive interval to remotely measure surface waves and the depth of the bubble layer created by surface wave breaking using a compact sonar, and 0-50KHz ambient sound with a passive hydrophone. The floats were programmed to repeat its dive interval every 4 hours.

Initial deployments were made in Hurricane Isidore in 2002 and Fabian in 2003. The more extensive 2004 deployments ahead of Hurricane Frances will be described here. The array

of floats and drifters (Fig. 14) was deployed from 20-23 UTC on Aug. 31, 2004 based on the Aug. 31, 03 UTC forecast for the 18 UTC, Sept. 1 storm position. The storm track passed just north of the shallow banks and islands north of Hispaniola. The array was therefore placed over deep water north of the storm track. The forecast proved to be extremely accurate, so that array elements passed under both the eye and maximum winds (60 ms^{-1}) of the storm.

The Hurricane Frances deployments clearly demonstrated the success of this new approach to measurement in hurricanes. The instruments were accurately targeted into the CAT 4 hurricane. All of the varieties of drifters and floats survived and worked successfully in this environment, with only minimal losses. Data was transmitted from the high wind region of the hurricane in nearly real time.

The buoys and floats revealed a warm anticyclonic eddy directly in the path of Frances, which was flanked by cooler cyclonic features. Sea surface height anomaly maps from satellite altimetry for the North Atlantic[2], such as the area along 30ºN east of northern Florida, sometimes referred to as the "Subtropical Convergence Zone", indicates the presence of an eddy-rich ocean in the vicinity of the storm track.

Parameterization of the air-sea fluxes that drive hurricanes depends on an understanding of the air-sea interface at high wind speeds. Figure 15 shows the ability of the floats to make detailed measurements of surface waves and near-surface bubble clouds across the hurricane. The time varying height of the sea surface was measured by the SOLO floats using an upward looking sonar compensated for the measured float depth. High frequency fluctuations in sea height yield measurements of the surface waves. Maximum significant wave height exceeded 10m. Intense breaking of these large waves injects bubbles into the ocean. The resulting near-

[2] See Atlantic map at http://www.aoml.noaa.gov/phod/cyclone/data/

surface bubble layer plays a key role in gas flux across the air-sea interface as well as having an important dynamical effect by changing the bulk density of the near-surface layer. Bubbles are very efficient sound scatterers, so that the thickness of the near-surface bubble layer can be measured by the upward looking sonar. Its thickness increases approximately as wind speed cubed, reaching a maximum thickness of over 10m. These results are confirmed by Lagrangian float measurements of conductivity, which decreases in the upper 10m due to bubbles.

Hurricanes draw their energy from the warm ocean waters. However, ocean mixing beneath a hurricane can significantly reduce sea surface temperatures from the pre-storm values. Fig. 16 shows the evolution of upper ocean potential density under the strongest winds of Hurricane Frances. It combines the vertical temperature profiles from an EM-APEX float with the nearby temperature measurements from the two Lagrangian floats. The EM-APEX floats also showed the evolution of the currents in the upper ocean (Sanford, et al., 2005). Fig 16 shows rapid deepening of the mixed layer and associated high shear across the thermocline. The strong wind and wave forcing directly generates turbulence in the upper 20-40m of the ocean. The Lagrangian floats are advected by the large-eddy velocities of this turbulence, repeatedly cycling across the turbulent layer and thereby tracing its depth and intensity (red and blue lines). Turbulent velocities are 0.1 ms^{-1} rms at the height of the storm, with the strongest downward vertical velocities reaching 0.3 ms^{-1}. The turbulent layer extends to 50m at the height of the storm. However, the changes in temperature indicate that mixing extends to 120 m (magenta line). Measurements of shear by the EM-APEX floats show (Fig. 17) a nearly critical Richardson number down to 120m, indicating a key role for shear instability in this deeper mixing. The one dimensional heat budget requires even deeper mixing as shown by the yellow dashed line (Fig. 16, bottom panel). A more detailed analysis indicates that horizontal heat

fluxes become important as the magenta and yellow-dashed lines diverge, indicating a transition of the boundary layer heat budget from vertical to three-dimensional.

The net effect of this strong ocean mixing is to cool the ocean surface, potentially reducing the enthalpy flux to the hurricane. The combined data from the floats and drifters is used to map the amount of cooling in Fig. 18. Cooling is most intense to the right of the storm center, with a cold wake spreading outward behind this region. The leading edge of this wake forms an SST front approximately 50 km wide which moves with the storm. The eye of storm is at the edge of this front, so that cooling at the eye is only about 0.5˚C compared to the maximum of 2.5˚C in a crescent-shaped pattern in the storm's right-rear quadrant, similar to that proposed by Black et al. (1988). SST gradients of up 2˚C exist across the inner 50 km of the storm, with a temperature range of about 27.5-30˚C. These data suggest that rather than specifying the SST at the hurricane inner core, it may be more useful to think in terms of the location of the SST front that exists beneath the core. Small changes in the location of this front relative to the core may have large effects on the enthalpy flux driving the storm.

6. SUMMARY AND CONCLUSIONS

The CBLAST hurricane program has yielded an unprecedented data set for exploring the coupled atmosphere and ocean boundary layers during an active hurricane. Key results from the analysis effort to date have increased the range of air-sea flux measurements significantly, which have allowed drag and enthalpy exchange coefficients to be estimated in wind speeds to nearly hurricane force. The drag coefficients (C_D's) estimated from this work suggest a leveling off with wind speed near 22-23 ms^{-1}, a considerably lower threshold than the 33 ms^{-1} value of Powell et al. (2003) and Donelan et al. (2004). This results in a extrapolated CD's for hurricane conditions

above 33 ms^{-1} of under 0.002, slightly lower than the results of Powell et al. (2003) and Donelan et al. (2004) for the 30 to 40 ms^{-1} wind speed interval, which are approximately .0022. The Dalton number is constant with wind speed up to hurricane force with a value of 0.00118, in close agreement with modified HEXOS and COARE 3.0 estimates. This results in a C_E/C_D ratio of approximately 0.7, somewhat less than the Emanuel threshold of 0.75 for hurricane development. Directional wave measurements made from the aircraft show distinctive characteristic as a function of storm-relative quadrant. Spectra range from tri-modal in the right-rear quadrant to bi-modal in the right front to unimodal in the left-front. The exchange coefficients appear independent of these wave spectral characteristics to within observational uncertainty. Boundary layer linear features (possible secondary circulations or 'roll' vortices) appear to characterize the boundary layer throughout the hurricane with their role in flux estimation yet to be determined.

The drifter and buoy deployments in Hurricanes Fabian (2003) and Frances (2004) were unqualified successes yielding first time ever observations of the 4-dimensional evolution of the subsurface ocean structure concurrent with airborne atmospheric boundary layer observations. The development of the cold wake behind Frances, showing a crescent-shaped pattern of cooling in the near-storm environment, was well observed with maximum cooling of 2.5 ºC. Shear at the base of the ocean mixed layer was found to develop quickly beneath the hurricane and meet the Richardson Number criteria of 1/4 for onset of turbulent mixing.

The analyses of this immense data set is ongoing. Incorporation into research and operational coupled models is just beginning. The outlook for major impacts on these modeling efforts is optimistic.

7. FUTURE PLANS FOR CBLAST HURRICANE

The analysis of CBLAST hurricane data sets has just begun. Continued support for analysis efforts is being provided by ONR and NOAA through the U.S. Weather Research Program (USWRP). Additional fundamental research will be ongoing in the years ahead for efforts such as merging 2D wave spectra from the SRA and the 1D wave spectra from the ARGO/SOLO floats to estimate the high frequency portion of the wave spectrum and its impact on air-sea fluxes in hurricanes. The impact of sea spray on air-sea enthalpy and momentum fluxes is yet to be demonstrated in hurricane winds, especially for major hurricanes of CAT 3 and above. Additional analysis is being carried out of the GPS sondes from the multi-sonde deployments in the hurricane eyewall for the purpose of estimating eyewall air-sea fluxes via budget calculations. From these, along with SFMR surface wind, SST and specific humidity estimates, additional C_D and C_E values will be estimated for extreme winds in excess of 50 ms^{-1}. Work will continue on the diagnoses of boundary layer linear features (possible secondary circulationsor 'roll vortices') and their role in air-sea fluxes including the variability by storm quadrant. Additional spectral analysis of BAT and LICOR turbulence flux data from along- and cross-wind flight legs as well analysis of IWRAP boundary layer wind profiles will help to address the vertical structure of this phenomenon in the hurricane PBL. Continued synthesis of drift buoy, float and satellite observations of ocean features in the path of Fabian and Frances will continue, including efforts to improve ocean mixing parameterizations in hurricane conditions.

Efforts to estimate fluxes at the top of the hurricane boundary layer will begin. Using the suite of BAT and LICOR turbulence instrumentation now available for both NOAA WP-3D aircraft, additional measurements will be sought over the coming years to fill gaps in the CBLAST data sets and to continue to focus on the parameterization with wind speed, wave

conditions and roll vortex effects. These observations will accompany new observations of sea spray droplets from any low level flights using the new suite of cloud microphysical spectrometer probes presently being improved on the P3 Aircraft- opening the possibility of extending sea spray studies.

The focus will also shift toward integrating existing and anticipated results on air-sea flux parameterization into high-resolution (1.7 km), coupled hurricane models such as Chen et al., 2006 (see box), as well as the new HWRF model, scheduled to become operational at the NOAA Environmental Prediction Center (EMC) during the 2006 hurricane season. EMC will also be examining the benefits of assimilating the profiling float data into their operational models to assess the value of deploying similar instruments in future storms to improve intensity predictions. Similarly, efforts are being made to integrate CBLAST results into the Navy NOGAPS and COAMPS models. Special efforts will begin to assess the impact of the new air-sea parameterization schemes on hurricane intensity.

We are at a unique point in history where airborne advanced technology is able to meet the requirements of the new generation of advanced coupled models for input and validation data in the hurricane, at the air-sea interface and in the ocean. Advances in hurricane computer modeling and observational technology are symbiotic. Continued investment in this effort now will produce large dividends at low risk for future improved hurricane intensity and track prediction.

Acknowledgements. The authors and team of CBLAST investigators wish to thank the Office of Naval Research for supporting this work as a Departmental Research Initiative, award numbers N00014-01-F-009 (Black, Drennan, French), N00014-01-1-0162 (Emanuel, Black), N00014-00-

1-0894 (Terrill, Melville), N00014-00-1-0893 (D'Asaro), N00014-02-1-0401 (Niiler) and N00014-01-F-0052 (Walsh). The United States Weather Research Program (USWRP) also supported Drennan with grant number NA17RJ1226. Walsh was also supported by the NASA Physical Oceanography Program. EM-APEX floats were developed with an ONR SBIR grant to Webb Research, Inc. We thank the NOAA Office of Oceanic and Atmospheric Research (OAR) for P3 flight hour and expendable dropsonde support for three years and to USWRP for CBLAST analysis support from 2005 to the present. Thanks are especially due to NOAA Deputy Assistant Administrator David Rogers for actively assisting in operational success of this experiment. We thank the NESDIS Ocean Winds project and lead PI Paul Chang (also a CBLAST PI) for the sharing of flight hour and dropsonde resources, without which the extensive effort over three years would have been impossible. We thank Frank Marks and the Hurricane Research Division staff for their infrastructure support for the NOAA aircraft field program effort, especially to Michael Black, Robert Rogers and Chris Landsea who served as Lead Project Scientist on many of the WP-3D flights. In particular, we thank Eric Uhlhorn of HRD, Alan Goldstein of AOC and Ivan Popstefanija of ProSensing, Inc. for their support of the Stepped Frequency Microwave Radiometer (SFMR) system during CBLAST flights. Special thanks is also due to James McFadden and the Aircraft Operations Center for their dedicated effort over four years to work with CBLAST PI's to test and install their instruments and in many cases to redesign their instruments for hurricane flight conditions. We especially thank Terry Lynch and Sean McMillan and the electrical engineering staff for their constant efforts to keep the computer and experimental hardware operating in hostile conditions and to Greg Bast and the aircraft flight engineer staff for their hard work to keep the aircraft in flight-ready status throughout the 3 years of active flights. Special thanks is due to Phil Hall, NOAA Corps, AOC

and ARL, for his extensive efforts to certify airworthiness for the BAT probe. We would also like to thank Phil Kennedy and the flight crews for the expert piloting and navigation of the aircraft. Thanks is especially due to Barry Damiano and Tom Shephard and the several flight directors who directed each CBLAST flight. Not one flight was cancelled and only one flight aborted due to mechanical problems. Special thanks is due to the 53rd Weather Reconnaissance Squadron of the Air Force Reserve Command for their extensive support of the buoy and float deployment effort, especially to Brig. Gen. Charles Ethredge and Gen. Richard Moss who served as outgoing and incoming AFRC 403rd Wing Commanders during 2003-2004. We would especially like to thank CMSgt. Robert E. Lee for supervising the air-drop training and bathroom renovations. Thanks to the many Air Force commands that participated in certifying the WC-130J, and individual platforms, to be deployed for airdrop capability. Finally special thanks is due to ONR CBLAST Program managers Simon Chang and Carl Friehe for actively helping to guide the program. Thanks is also extended to Scott Sandgathe, Steve Tracton, Linwood Vincent, Theresa Paluszkiewicz and Ron Ferek for ONR management support. The assistance of Susanne Lehner, DLR Germany and U.Miami in analysis of RADARSAT imagery is acknowledged.

References

Andreas, E. L. and K. A. Emanuel, 2001: Effects of Sea Spray on Tropical Cyclone Intensity. *J. Atmos. Sci.*, **58**, 3741–3751.

Bell, M. M. and M. T. Montgomery, 2006: Observed structure, evolution and potential intensity of category five Hurricane Isabel (2003) from 12 – 14 September. Submitted to *Mon. Wea. Rev.*

Black, P. G., R. L. Elsberry and L. K. Shay, 1988: Airborne surveys of Ocean Current and temperature perturbations induced by hurricanes. *Adv. Underwater Technol., Ocean Sci. Engineer.*, **16**, 51-58.

Chen, S. S., J. F. Price, W. Zhao, M. A. Donelan, E. J. Walsh, and H. L. Tolman, 2006: The CBLAST hurricane program and the next generation fully coupled atmosphere-wave-ocean models for hurricane research and prediction. Submitted to *BAMS.*D'Asaro, E.A., 2003: Performance of autonomous Lagrangian floats. *J. Atmos. Oceanic Technol.*, 20, 896-911.

DeCosmo, J., K. B. Katsaros, S. D. Smith, R. J. Anderson, W. A. Oost, K. Bumke, and H. Chadwick, 1996: Air-sea exchange of water vapor and sensible heat: The humidity exchange over the sea (HEXOS) results. *J. Geophys. Res.,* **101** (C5), 12001-12016.

DeMaria, M., M. Mainelli, L.K. Shay, J.A. Knaff, and J. Kaplan, 2005: Further Improvements to the Statistical Hurricane Intensity Prediction Scheme (SHIPS), Wea. Forecasting, 20, 531-543.

Donelan, M. A., 1990: Air-Sea Interaction, *The Sea: Ocean Engineering Science*, B. LeMéhauté and D. Hanes, Eds., Vol. 9, John Wiley and Sons, New York, pp. 239-292.

Donelan, M. A., B. K. Haus, N. Reul, W. J. Plant, M. Stianssnie, H. C. Graber, O. B. Brown, E. S. Saltzman, 2004: On the limiting aerodynamic roughness of the ocean in very strong winds. *Geophys. Res. Lett.*, **31,** L18306.

Drennan, W. M., J. Zhang, J. R. French, C. McCormick and P. G. Black, 2006: Turbulent fluxes in the hurricane boundary layer, II. Latent heat flux, *J. Atmos. Sci.*, submitted.

Edson, J., T. Crawford, J. Crescenti, T. Farrar, J. French, N. Frew, G. Gerbi, C. Helmis, T. Hristov, D. Khelif, A. Jessup, H. Jonsson, M. Li, L. Mahrt, W. McGillis, A.

Plueddemann, L. Shen, E. Skyllingstad, T. Stanton, P. Sullivan, J. Sun, J. Trowbridge, D. Vickers, S. Wang, Q. Wang, R. Weller, J. Wilkin, D. Yu, and C. Zappa, 2006: The Coupled Boundary Layers and Air-Sea Transfer Experiment in Low Winds (CBLAST-LOW). Submitted to *BAMS*.

Emanuel, K. A., 1986: An Air-Sea Interaction Theory for Tropical Cyclones. Part I: Steady-State Maintenance. *J. Atmos. Sci.*, **43**, 585–605.

Emanuel, K. A., 1995: Sensitivity of tropical cyclones to surface exchange coefficients and a revised steady-state model incorporating eye dynamics. *J. Atmos. Sci.*, **52,** 3969-3976.

Emanuel, K. A., 2005: Increasing destructiveness of tropical cyclones over the past 30 years. *Nature*, **436**, 686-688.

Esteban-Fernandez, D., S. Frazier, J. Carswell, P. Chang, P. Black and F. Marks, 2004: 3-D atmospheric boundary layer wind fields from Hurricanes Fabian and Isabel. *26th Conf. on Hurr. and Tropical Meteorol.*, AMS, Miami Beach, FL.

Fairall, C. W., E. F. Bradley, J. E. Hare, A. A. Grachev and J. B. Edson, 2003: Bulk parameterization of air-sea fluxes: updates and verification for the COARE algorithm. *J. Climate*, **16**, 571-591.

Foster, R. C., 2005: Why rolls are prevalent in the hurricane boundary layer. *J. Atmos. Sci.*, **62**, 2647-2661.

Franklin, J.L., C. J. McAdie, and M. B. Lawrence. 2003: Trends in Track Forecasting for Tropical Cyclones Threatening the United States, 1970–2001. Bull. Amer. Meteor. Soc., 84, 1197–1203.

French, J.R., W.M. Drennan, J. Zhang, and P.G. Black, 2006: Turbulent Fluxes in the Hurricane Boundary Layer, I. Momentum Flux. Submitted to *Journal of Atmospheric Science*.

Goldenberg, S.B., C.W. Landsea, A. M. Mestas-NuÑez, W. M. Gray, 2001: The Recent Increase in Atlantic Hurricane Activity: Causes and Implications. *Science* 293, 474-478.

Hebert, P. J., 1976: Atlantic hurricane season of 1975. *Mon. Wea. Rev.*, **104**, 453-475.

Katsaros, K. B., P. W. Vachon, W. T. Liu, and P. G. Black, 2002: Microwave remote sensing of tropical cyclones from space. *J. Oceanogr.*, **58,** 137-151.

Kleiss, J. M., W. K. Melville, J. R. Lasswell, P. Matusov and E. Terrill, 2004: Breaking waves in hurricanes Isabel and Fabian. *26th Conf. on Hurr. and Tropical Meteorol.*, AMS, Miami Beach, FL.

Large, W. G., and S. Pond, 1981: Open ocean momentum flux measurements in moderate to strong winds. *J. Phys. Oceanogr.*, **11,** 324-336.

Landsea, C.W., 2005: Hurricanes and global warming. *Nature*, **438**, E11-E12.

Lorsolo, S. and J. R. Schroeder, 2006a: Small scale features observed in the boundary layer of Hurricanes Isabel (2003) and Frances (2004). Proc. Air-Sea Interaction Conf., AMS, Atlanta, GA.

Lorsolo, S. and J. R. Schroeder, 2006b: Tower and Doppler radar observations from the boundary layers of Hurricanes Isabel (2003) and Frances (2004). Proc. 27th Conference on Hurricanes and Tropical Meteorology, AMS, Monterey, CA.

Montgomery, M. T., M. M. Bell, S.Aberson, and M. Black, 2006: Hurricane Isabel (2003): New insights into the physics of intense storms. Part I. Mean vortex structure and maximum intensity estimate. Accepted, *Bull. Amer. Meteorol. Soc.*

Morrison, I., S. Businger, F. Marks, P. Dodge and J. Businger, 2005: An observational case for the prevalence of roll vortices in the hurricane boundary layer, *J. Atmos. Sci*. **62**, 2662-2673

.Moss, M. S., 1978: Low-Level Turbulence Structure in the Vicinity of a Hurricane, *Mon. Wea. Rev.*, **106**, 841–849.

Moss, M. S. and F. J. Merceret, 1977: A Comparison of Velocity Spectra from Hot Film Anemometer and Gust-Probe Measurements, *J. Appl. Meteorol.*,**16**, 319–320.

Moss, M. S. and F. J. Merceret, 1976: A Note on Several Low-Layer Features of Hurricane Eloise (1975), *Mon. Wea. Rev.*, **104**, 967–971.

Nystuen, J. A. and H. D. Selsor, 1997: Weather classification using passive acoustic drifters. *J. Atmos. and Oceanic Tech.*, **14**, 656-666.

Powell, M. D., and S. H. Houston, 1996: Hurricane Andrew's Landfall in South Florida. Part II: Surface Wind Fields and Potential Real-time Applications. *Weather. Forecast.*, **11**, 329-349.

Powell, M. D., S. H. Houston, L. R. Amat, and N Morisseau-Leroy, 1998: The HRD real-time hurricane wind analysis system. *J.Wind Engineer. and Indust. Aerodyn*. **77&78**, 53-64.

Powell, M. D., and S. H. Houston, 1998: Surface wind fields of 1995 Hurricanes Erin, Opal, Luis, Marilyn, and Roxanne at landfall. *Mon Wea. Rev.*, **126**, 1259-1273.

Powell, M. D., P. J. Vickery, and T. A. Reinhold, 2003: Reduced drag coefficient for high wind speeds in tropical cyclones. *Nature*, **422**, 279-283.

Sanford, T. B., J. H. Dunlap, J. A. Carlson, D. C. Webb and J. B. Griton, 2005: Autonomous Velocity and Density Profiler: EM-APEX. Proceedings of the IEEE/OES Eighth Working Conference on Current Measurement Technology, IEEE Cat No. 05CH37650, ISBN: 0-7803-8989-1, pp. 152-156

Smith, S. D., 1980: Wind stress and heat flux over the ocean in gale force winds. *J. Phys. Oceanogr.*, **10,** 709-726.

Smith, S.D., R.J. Anderson, W.A. Oost, C. Kraan, N. Maat, J. DeCosmo, K.B. Katsaros, K.L. Davidson, K. Bumke, L. Hasse and H.M. Chadwick, 1992: Sea surface wind stress and drag coefficients: the HEXOS results. *Bound. Layer Meteorol*. **60**, 109-142.

Uhlhorn, E. W., and P. G. Black, 2003: Verification of remotely sensed sea surface winds in hurricanes. *J. Atmos. Ocean. Technol.,* **20,** 99-116.

Uhlhorn, E. W., P. G. Black, J. L. Franklin, M. Goodberlet, J. Carswell, and A.S. Goldstein, 2006: Hurricane surface wind measurement from an operational Stepped Frequency Microwave Radiometer. Submitted *Wea. And Forecasting*.

Webster, P. J., G. J. Holland, J. A. Curry, H.-R. Chang, 2005: Changes in Tropical Cyclone Number, Duration, and Intensity in a Warming Environment. *Science,* **309**, 1844-1846.

Wright, C. W., E. J. Walsh, D. Vandemark, W. B. Krabill, S. H. Houston, M. D. Powell, P. G. Black, and F. D. Marks, 2001: Hurricane directional wave spectrum spatial variation in the open ocean. *J. Phys. Oceanogr.,* **31,** 2472-2488.

Wurman, J. and J. Winslow, 1998: Intense sub-kilometer scale boundary layer rolls observed in Hurricane Fran. Science, **280**, 555-557.

Wurman, J, C. Alexander, P. Robinson and F. Masters, 2006: Preliminary comparisons of DOW and insitu measurements in Hurricane Rita. Proc. 27th Conference on Hurricanes and Tropical Meteorology, AMS, Monterey, CA.

Yelland, M.J., B.I. Moat, P.K. Taylor, R.W. Pascal, J. Hutchings and V.C. Cornell, 1998: Wind stress measurements from the open ocean corrected for airflow distortion by the ship. *J. Phys. Oceanogr.* **28**, 1511-1526.

Table 1a. CBLAST Hurricane PI Team: functions and observable quantities, instrumentation and principal investigators (PIs)- **Aircraft Component**

No	Function	Instrument	PI	Affiliation
1	Chief Scientist, Flight Planning, Program Coordination	All	Peter Black	NOAA/AOML/HRD
2	Ocean Winds Lead Scientist, Sfc Wind Vector, SATCOM, Satellite Applications	IWRAP	Paul Chang	NOAA/NESDIS/ORA
3	Dropsondes, SST, Sfc Wind Speed	GPS sonde, AXBT, SFMR	Peter Black, Eric Uhlhorn	NOAA/AOML/HRD
4	Sea spray, particle spectrometer	CIP	Chris Fairall	NOAA/ESRL/ETL
5	Sea spray, particle velocimeter	PDA	William Asher	U. Washinton/APL
6	Extreme wind sfc flux, theory	Dropsonde	Kerry Emanuel	MIT
7	Surface waves	SRA	Ed Walsh	NASA/Goddard
8	Momentum, sensible heat flux	BAT	Jeff French	NOAA/ARL; U. Wyoming
9.	Moisture flux	LICOR	William Drennan	U. Miami/ RSMAS/AMP
10.	Surface wind vector, continuous PBL wind profiles	IWRAP, USFMR	Stephen Frasier, James Carswell, Daniel Esteban, Rob Contreras	UMASS/ MIRSL
11.	Surface wave breaking, foam coverage	ScrippsVIS, IR camera	Ken Melville, Eric Terrill	UCSD/SCRIPPS

Table 1b. CBLAST Hurricane PI Team: functions and observable quantities, instrumentation and principal investigators (PIs)- **Drifter/ Float Component**

No	Function	Instrument	PI	Affiliation
1	Ocean mixing, gas exchange	Lagrangian floats	Eric D'Asaro	U. Washington/APL
2	Ocean current, temperature and salinity profiling	EM-APEX floats	Tom Sanford	U. Washington/APL
3	Ocean acoustics, surface waves, ocean temperature profiles	ARGO/SOLO floats	Eric Terrill	UCSD/SCRIPPS
4	SST, Sfc wind vector, ocean acoustics, surface air pressure	SVP/ADOS drifters	Peter Niiler, William Scuba Jan Morzel	UCSD/SCRIPPS
5	Satellite ocean heat content, buoy archive	Satellite altimeters	Gustavo Goni	NOAA/AOML/PHOD

Table 2: List of acronyms

ADOS	Autonomous Drifting Ocean Stations
AFRC	Air Force Reserve Command
AOC	Aircraft Operations Center
AOML	Atlantic Oceanographic and Meteorological Laboratory
APL	Applied Physics Laboratory
AXBT	Airborne EXpendable Bathythermograph
BAT	Best Aircraft Turbulence (probe)
CAT	Hurricane CATegory
CAMEX	Convection And Moisture Experiment
CBLAST	Coupled Boundary Layer Air-Sea Transfer
CIP	Cloud Imaging Probe
COAMPS	Coupled Ocean Atmosphere Mesoscale Prediction System
COARE	Coupled Ocean-Atmosphere Response Experiment
DOW	Doppler on Wheels
DSD	Drop Size Distribution
EM-APEX	Electro-Magnetic Autonomous Profiling EXplorer
EMC	Environmental Modeling Center
ETL	Environmental Technology Laboratory
FRD	Field Research Division
FSSP	Forward Scattering Spectrometer Probe
HEXOS	Humidity EXchange Over the Sea
HFPP	Hurricane Field Program Plan
HRD	Hurricane Research Division
HWRF	Hurricane Weather Research and Forecasting
IWRAP	Integrated Wind and Rain Atmospheric Profiler
NESDIS	National Environnemental Satellite Data Information Service
NOGAPS	Navy Operational Global Atmospheric Prediction System
NRL	Naval Research Laboratory
OAR	Office of Oceanic and Atmospheric Research
ONR	Office of Naval Research
PDA	Precipitation Detection Algorithm
PHOD	PHysical Oceanography Division
RSMAS	Rosenstiel School of Marine and Atmospheric Science
SAR	Synthetic Aperture Radar
SATCOM	SATellite COMmunications (system)
SBIR	Small Business Innovative Research (program)
SFMR	Stepped Frequency Microwave Radiometer
SOLO	Sounding Oceanographic Lagrangian Observer
SRA	Scanning Radar Altimeter
TA	TAil (airborne Doppler radar)

TOGA	Tropical Ocean Global Atmosphere
UM	University of Miami
UMASS	University of Massachusetts
UNOLS	University-National Oceanographic Laboratory System
USFMR	Umass Simultaneous Frequency Microwave Radiometer
USWRP	United States Weather Research Program
UW	University of Washington
WRS	Weather Reconnaissance Squadron

Table 3 –Oceanographic Platforms Deployed in CBLAST Hurricane

	MiniMet	**ADOS**	**EM-APEX**	**Lagrangian**	**SOLO**
Type	Drifter	Drifter	Float	Float	Float
Measurements	SST Air Pressure Wind Speed Wind direction Position	SST Air Pressure Wind Speed Wind Direction Temperature 0-120m Position	Temperature Salinity Pressure Velocity Position	Temperature Salinity Pressure Gas Tension Oxygen Position	Temperature Salinity Pressure Oxygen Sound 0-50kHz Wave height Position
Satellite	Argos	Argos	Iridium	Iridium	Orbcomm
2003 Deployed	16			4	2
2004 Deployed	30	8	3	2	9

Figure Captions

Figure 1. CBLAST survey pattern showing planned expendable probe deployments along a 'figure 4' pattern relative to the storm's eyewall and rainband features. Location of planned stepped-descent patterns to measure boundary layer fluxes is shown schematically. IP is the initial point in the pattern, and FP is the final point.

Figure 2. Vertical alignment of stepped descent flight legs along with expendable probe location along the 25 nmi (46 km) leg length.

Figure 3. Location of the BAT turbulence probe and LICOR fast response humidity probe on the WP-3D aircraft.

Figure 4. CBLAST stepped descent flight patterns flown in Hurricanes Fabian and Isabel in 2003, plotted in storm-relative coordinates, with the storm motion indicated by the arrow (up). Circles are shown at 100 km intervals. Flight tracks are superimposed on NASA MODIS visual image of Hurricane Isabel on 14 Sept, 2003 at 1445 UTC. In addition a WP-3D Lower Fuselage (LF) airborne radar image from NOAA 43 of Isabel at 1642 UTC is overlaid indicating typical eyewall and rainband structure. MODIS image courtesy of MODIS Rapid Response Project at NASA/GSFC.

Figure 5. Drag coefficient estimates derived from CBLAST stepped-descent flight legs in Hurricanes Fabian and Isabel (2003). The asterisks represent average values in 2.5 ms^{-1} bins, and the bars show 95% confidence intervals. The squares are from flight

legs in the right-front quadrant of the storms, the plus signs from the right-rear quadrant and the diamonds from the left-front quadrant. The blackdash-dot line represents the values from Donelan et al. (2004); the red dash-dot line from Powell et al. (2003); blue-dashed line from an average of Smith (1980) and Large and Pond (1981); the red-dashed line from Yelland et al. (1998); black dashed line from HEXOS (Smith et al. 1992), and the grey circles from CBLAST-Low (Edson et al. 2006).

Figure 6. Moisture exchange coefficient (Dalton Number) estimates derived from CBLAST stepped-descent flight legs in Hurricanes Fabian and Isabel (2003). The asterisks represent average values in 2.5 ms^{-1} bins, and the bars show 95% confidence limits. The squares are from flight legs in the right-front quadrant of the storms, plus signs from the right-rear quadrant and diamonds from the left-front quadrant. The black dashed line represents the HEXOS line (DeCosmo et al. 1996), modified as per Fairall et al. (2003) and extended to 36 ms^{-1}. The green solid line is the COARE 3.0 curve (Fairall et al. 2003), and the grey circles are from CBLAST-Low (Edson et al. 2006).

Figure 7. Ratio of C_E/C_D derived from CBLAST measurements. The asterisks represent average values in 2.5 ms^{-1} bins, and the bars show 95% confidence limits. The black dashed curve is the mean ratio from HEXOS (DeCosmo et al. 1996, modified as per Fairall et al. 2003; Smith et al. 1992). The solid green line is the ratio values from COARE 3.0 (Fairall et al. 2003). The grey circles are from CBLAST-Low

(Edson et al. 2006). The dash-dot horizontal magenta line is the 0.75 threshold for TC development proposed by Emanuel (1995).

Figure 8. Swath of wave elevations from SRA from 200 m flight altitude during Fabian, 2003. Scale of aircraft is shown at 1 km along track, 0.2 km cross track position.

Figure 9. Analysis of SRA primary swell direction of propagation (solid black 'streamlines'), wave height in meters (dashed black contours) and wave steepness x 10^{-3} (thin solid blue contours) for Hurricane Bonnie, August 24, 1998 at 2052 UTC. Measurements made at an aircraft altitude of 1550 m. Asymmetric convective radar reflectivity contours in dBz are: green- 28, yellow- 35, red- 41 and white- 48. Storm is divided into three sectors according to wave directional characteristics: I. Unimodal, short wavelength (~150-200m) waves moving with the wind, II. Bi-modal or tri-modal spectra shifting to longer wavelengths (~200-300m) with dominant waves moving outward by up to 45 deg, relative to the wind direction and III. Unimodal spectra with peak long-wavelength waves (~300-350 m) moving outward relative to the wind by 60 to 90 deg. Direction of storm motion is indicated by the bold dashed arrow.

Figure 10. The center of the figure shows wind speed contours (ms-1) from the HRD H*WIND surface wind analysis- based mainly on SFMR surface wind speed measurements in Hurricane Ivan at 2230 UTC on 14 September 2004 for a 2° box in latitude and longitude centered on the eye. Arrow at the center indicates Ivan's

direction of motion (330º). The storm-relative locations of twelve 2D surface wave spectra measured by the SRA are indicated by the black dots. The spectra have nine solid contours linearly spaced between the 10% and 90% levels relative to the peak spectral density. The dashed contour is at the 5% level. The outer solid circle indicates a 200 m wavelength and the inner circle indicates a 300 m wavelength. The dashed circles indicate wavelengths of 150, 250, and 350 m (outer to inner). The thick line at the center of each spectrum points in the downwind direction, with its length proportional to the surface speed. The upper number at the center of each spectrum is the significant wave height and the lower number is the distance from the center of the eye. The average radial distance for the twelve spectral locations is 80 km. The SRA data which produced the spectra were collected between 2030 UTC on 14 September and 0330 UTC on 15 September.

Figure 11. RADARSAT SAR image (top) from right-front quadrant of Hurricane Fran, similar to that obtained for Hurricane Isidore, 2002. The horizontal scale is 200 km. Histogram (bottom) of wind streak wavelengths from analyzed RADARSAT image of Hurricane Isidore, 23 September, 2002. Arrow indicates peak in aircraft-derived spectrum in Fig. 12. RADARSAT image courtesy of Canadian Space Agency.

Figure 12. Co-spectrum of vertical momentum flux (-u'w') along a 120 m altitude radial flight leg into Hurricane Isidore, 22 September, 2002. The true air speed is 110 ms^{-1}.

Figure 13. Drawings of the three varieties of floats and a surface drifter as deployed into

Hurricane Frances. Schematic depicts operations in Hurricane Frances (2004).

Figure 14. Hurricane Frances (2004) float and drifter array. Heavy line shows storm track, labeled by Julian Day (JD 245.00 = 1 Sept., 00 UTC). Colors indicate type of instrument. Instrument tracks are plotted from deployment on JD 244 (31 Aug) to JD 246.5 (2 Sept, 12 UTC). Deployment position is indicated by black symbol.

Figure 15. Significant surface wave height and bubble cloud depth measured by the 9 SOLO floats and wind speed at the float location from H*WIND analysis. Time axis is hours from time of maximum wind at each float.

Figure 16. Evolution of the density structure of the upper ocean near the radius of maximum winds of Hurricane Frances. a) Wind speed and atmospheric pressure from HRD H*WIND analysis at the two Lagrangian floats. b) Potential density contours (kg m^{-3}) in black, trajectories of Lagrangian floats in red and blue, measured depth of the mixed layer in magenta and estimated depth of the mixed layer from a vertical heat budget in yellow (dashed).

Figure 17. EM-APEX float 1633 located 50 km to the right of storm track in highest winds. The upper two panels are of East (U) and North (V) velocity components versus depth and time with the 29 and 25ºC isotherms in bold with a contour interval of 0.5ºC. The center of the storm passed at approximately 1700 UTC on Sept 1.

Ocean Heat Content (OHC) is shown for water warmer than 26ºC and shallower than 180 m. The bottom panel is 'reduced shear', a stability parameter, with the temperature contours superimposed. This quantity is related to the Richardson number, $Ri=N^2/S^2$, where N is the Brunt-Väisälä frequency and S is the vertical current shear. A necessary condition for shear instability is $N^2/S^2 < 1/4$. This instability criteria is re-written as $S^2 - 4N^2 > 0$ to indicate where mixing is possible. The quantity $S^2 - 4N^2$ is contoured in the bottom panel with the green, yellow and red colors indicating where the instability criteria is equaled or exceeded. The blue colors indicate stable conditions less than zero.

Figure 18. SST decreases (C) beneath hurricane Frances (2003) in storm-centered coordinate system. White dots show storm-relative locations of float and drifter data. Storm motion is to left. Colors show mapped SST change from pre-storm value. Contours show wind speed in ms^{-1} from H*WIND analysis. Storm positions are in increments of one-quarter Julian Days (JD), or 6 hours, where JD 245 is Sept 1.

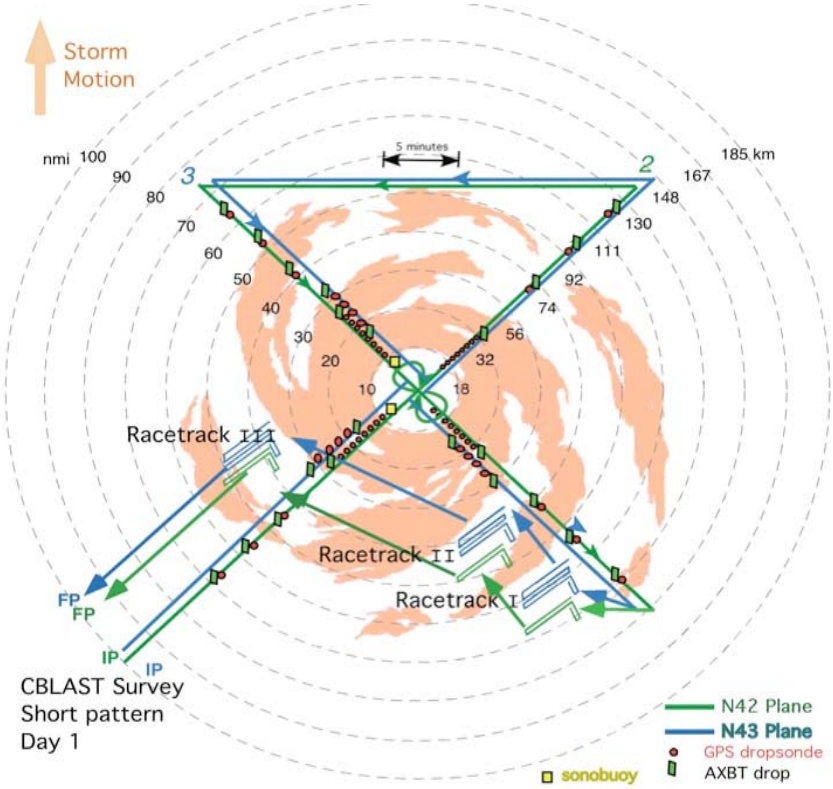

Figure 3. CBLAST survey pattern showing planned expendable probe deployments along a 'figure 4' pattern relative to the storm's eyewall and rainband features. Location of planned stepped-descent patterns to measure boundary layer fluxes is shown schematically. IP is the initial point in the pattern, and FP is the final point.

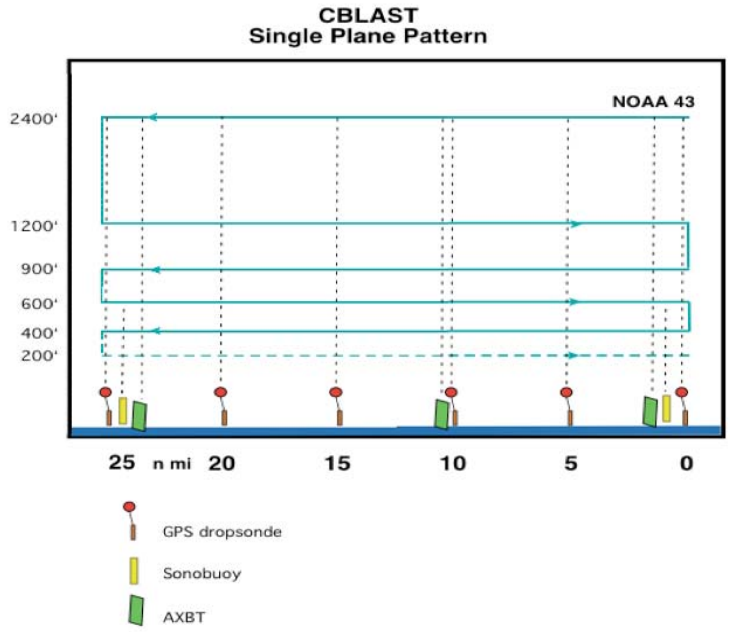

Figure 4. Vertical alignment of stepped descent flight legs along with expendable probe location along the 25 nmi (46 km) leg length.

Figure 3. Location of the BAT turbulence probe and LICOR fast response humidity probe on the WP-3D aircraft.

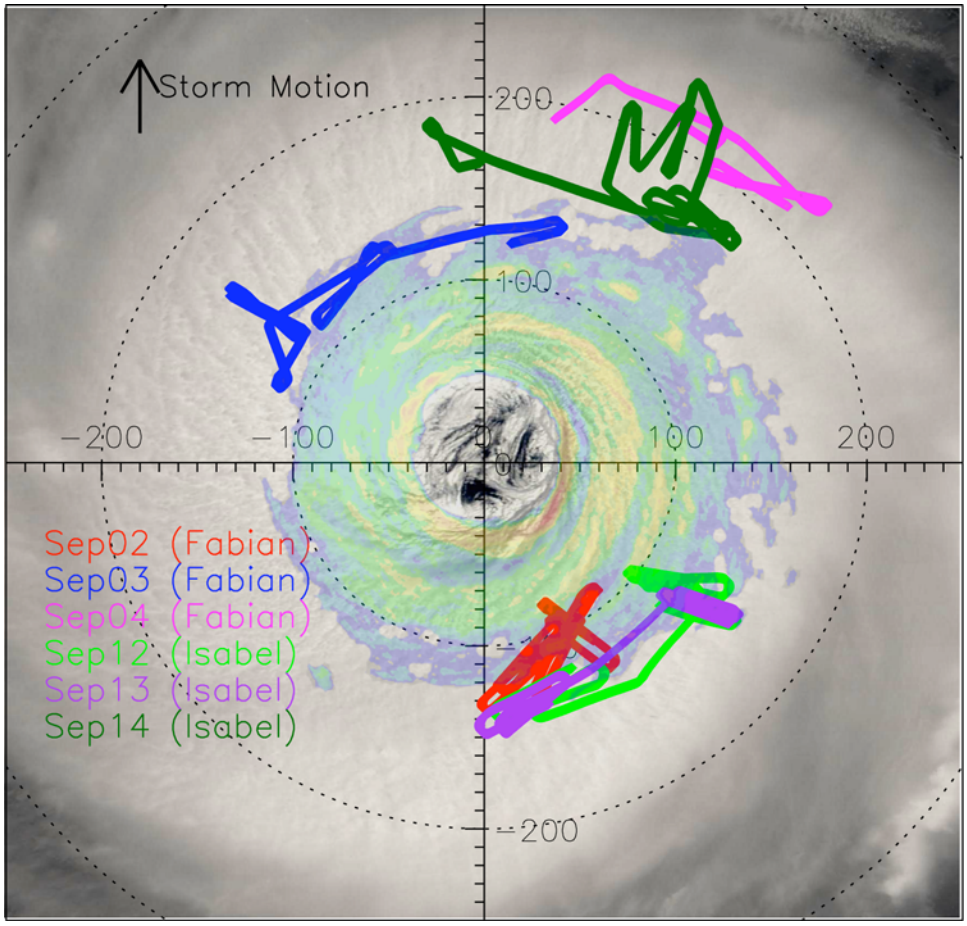

Figure 4. CBLAST stepped descent flight patterns flown in Hurricanes Fabian and Isabel in 2003, plotted in storm-relative coordinates, with the storm motion indicated by the arrow (up). Circles are shown at 100 km intervals. Flight tracks are superimposed on NASA MODIS visual image of Hurricane Isabel on 14 Sept, 2003 at 1445 UTC. In addition a WP-3D Lower Fuselage (LF) airborne radar image from NOAA 43 of Isabel at 1642 UTC is overlaid indicating typical eyewall and rainband structure. MODIS image courtesy of MODIS Rapid Response Project at NASA/GSFC.

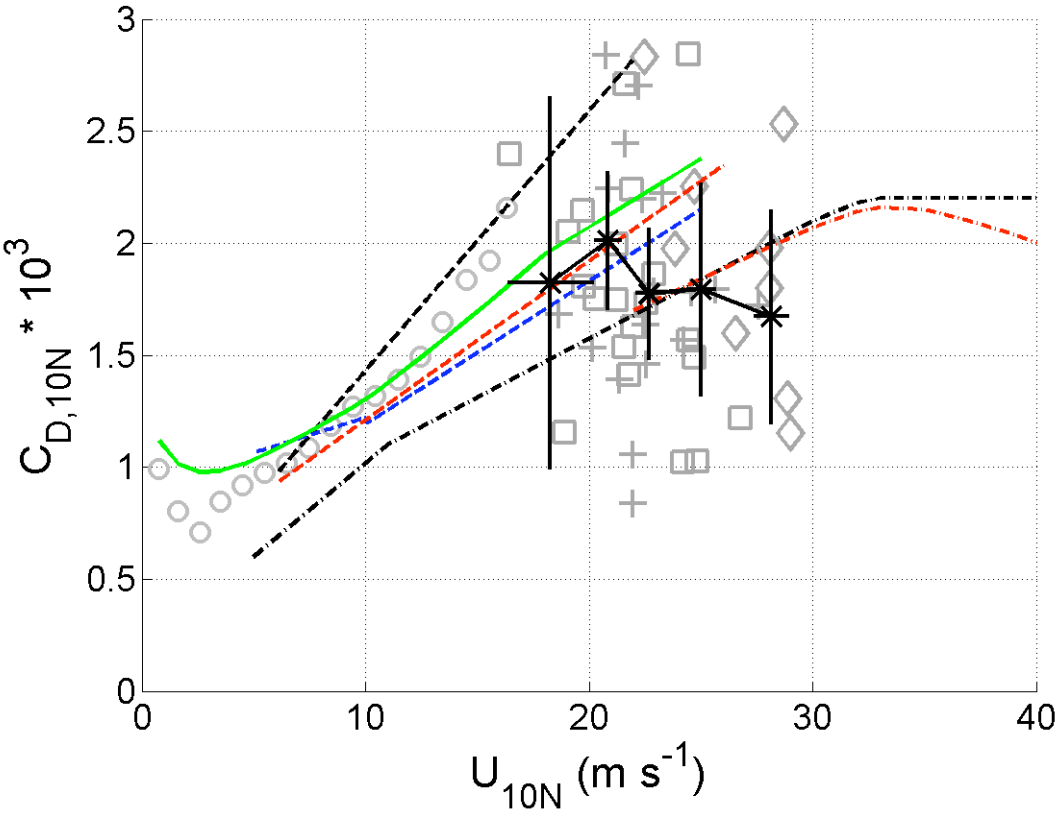

Figure 5. Drag coefficient estimates derived from CBLAST stepped-descent flight legs in Hurricanes Fabian and Isabel (2003). The asterisks represent average values in 2.5 ms^{-1} bins, and the bars show 95% confidence intervals. The squares are from flight legs in the right-front quadrant of the storms, the plus signs from the right-rear quadrant and the diamonds from the left-front quadrant. The blackdash-dot line represents the values from Donelan et al. (2004); the red dash-dot line from Powell et al. (2003); blue-dashed line from an average of Smith (1980) and Large and Pond (1981); the red-dashed line from Yelland et al. (1998); black dashed line from HEXOS (Smith et al. 1992), and the grey circles from CBLAST-Low (Edson et al. 2006).

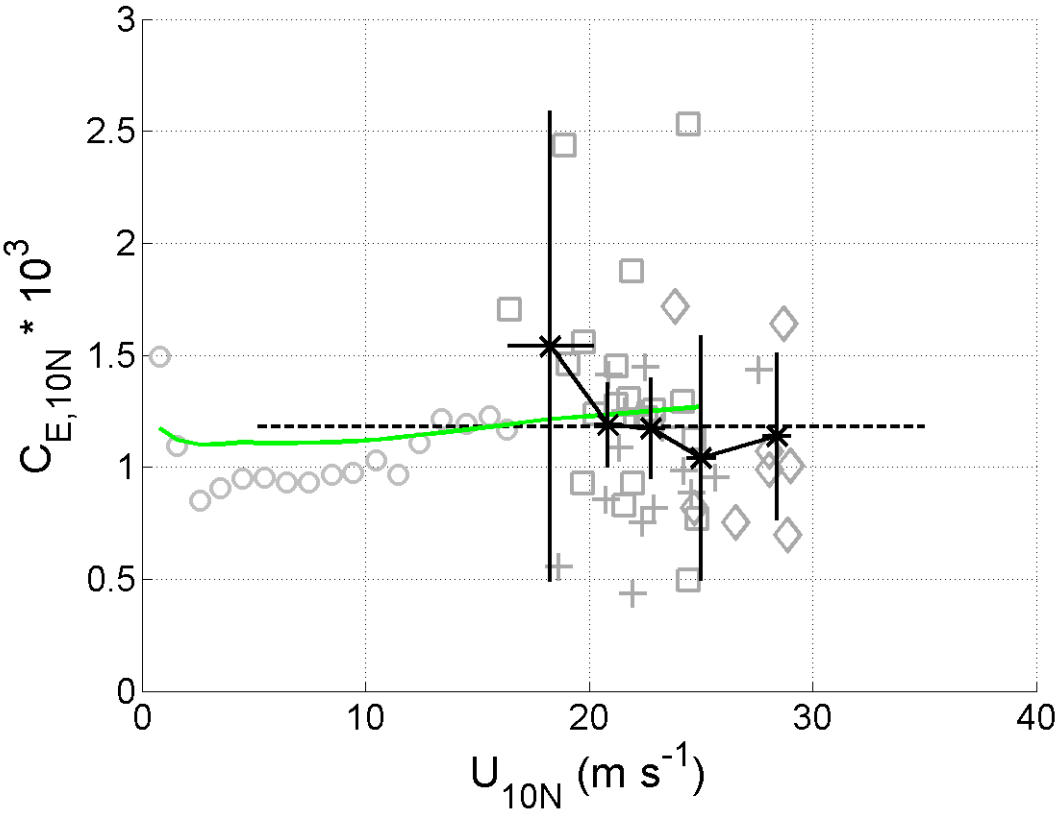

Figure 6. Moisture exchange coefficient (Dalton Number) estimates derived from CBLAST stepped-descent flight legs in Hurricanes Fabian and Isabel (2003). The asterisks represent average values in 2.5 ms^{-1} bins, and the bars show 95% confidence limits. The squares are from flight legs in the right-front quadrant of the storms, plus signs from the right-rear quadrant and diamonds from the left-front quadrant. The black dashed line represents the HEXOS line (DeCosmo et al. 1996), modified as per Fairall et al. (2003) and extended to 36 ms^{-1}. The green solid line is the COARE 3.0 curve (Fairall et al. 2003), and the grey circles are from CBLAST-Low (Edson et al. 2006).

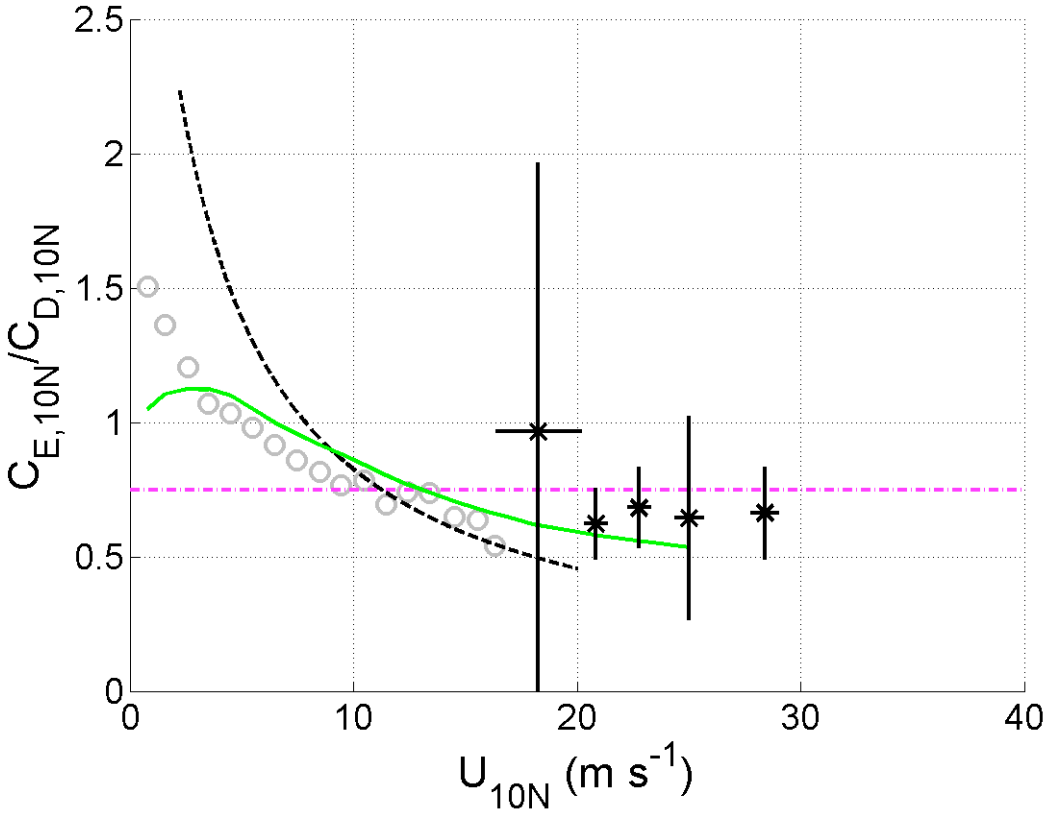

Figure 7. Ratio of C_E/C_D derived from CBLAST measurements. The asterisks represent average values in 2.5 ms^{-1} bins, and the bars show 95% confidence limits. The black dashed curve is the mean ratio from HEXOS (DeCosmo et al. 1996, modified as per Fairall et al. 2003; Smith et al. 1992). The solid green line is the ratio values from COARE 3.0 (Fairall et al. 2003). The grey circles are from CBLAST-Low (Edson et al. 2006). The dash-dot horizontal magenta line is the 0.75 threshold for TC development proposed by Emanuel (1995).

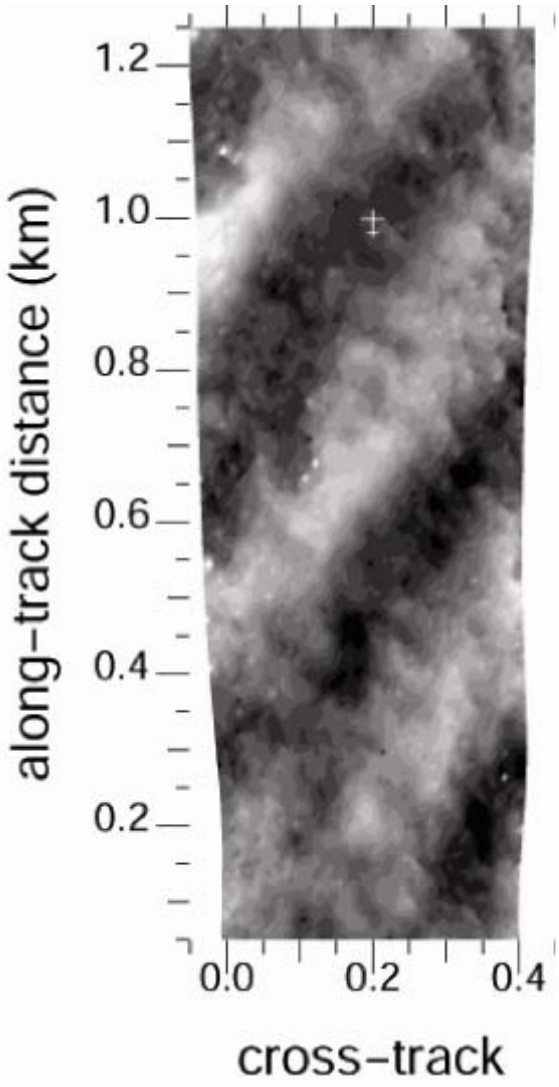

Figure 8. Swath of wave elevations from SRA from 200 m flight altitude during Fabian, 2003. Scale of aircraft is shown at 1 km along track, 0.2 km cross track position.

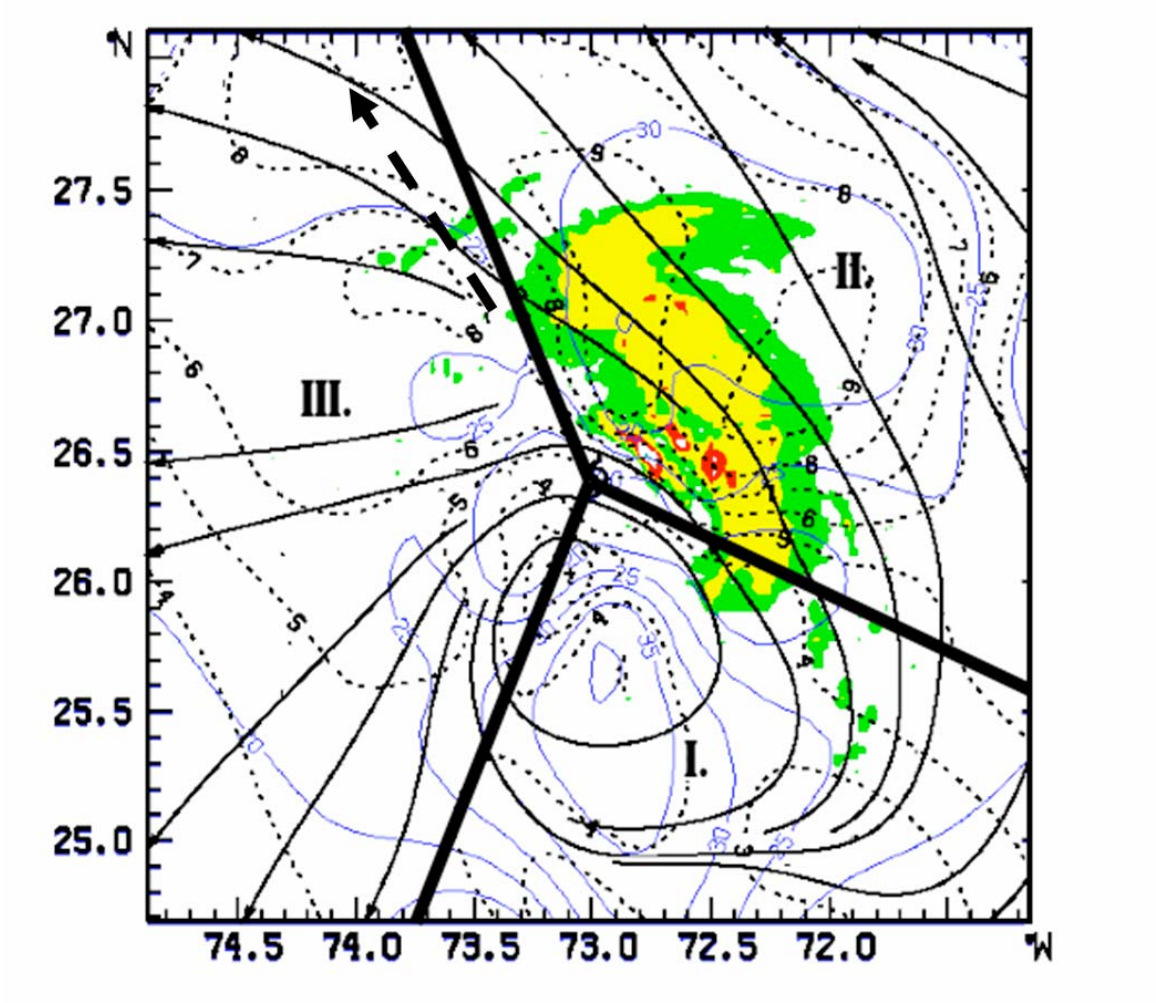

Figure 9. Analysis of SRA primary swell direction of propagation (solid black 'streamlines'), wave height in meters (dashed black contours) and wave steepness x 10^{-3} (thin solid blue contours) for Hurricane Bonnie, August 24, 1998 at 2052 UTC. Measurements made at an aircraft altitude of 1550 m. Asymmetric convective radar reflectivity contours in dBz are: green- 28, yellow- 35, red- 41 and white- 48. Storm is divided into three sectors according to wave directional characteristics: I. Unimodal, short wavelength (~150-200m) waves moving with the wind, II. Bi-modal or tri-modal spectra shifting to longer wavelengths (~200-300m) with dominant waves moving outward by up to 45 deg, relative to the wind direction and III. Unimodal spectra with peak long-wavelength waves (~300-350 m) moving outward relative to the wind by 60 to 90 deg. Direction of storm motion is indicated by the bold dashed arrow.

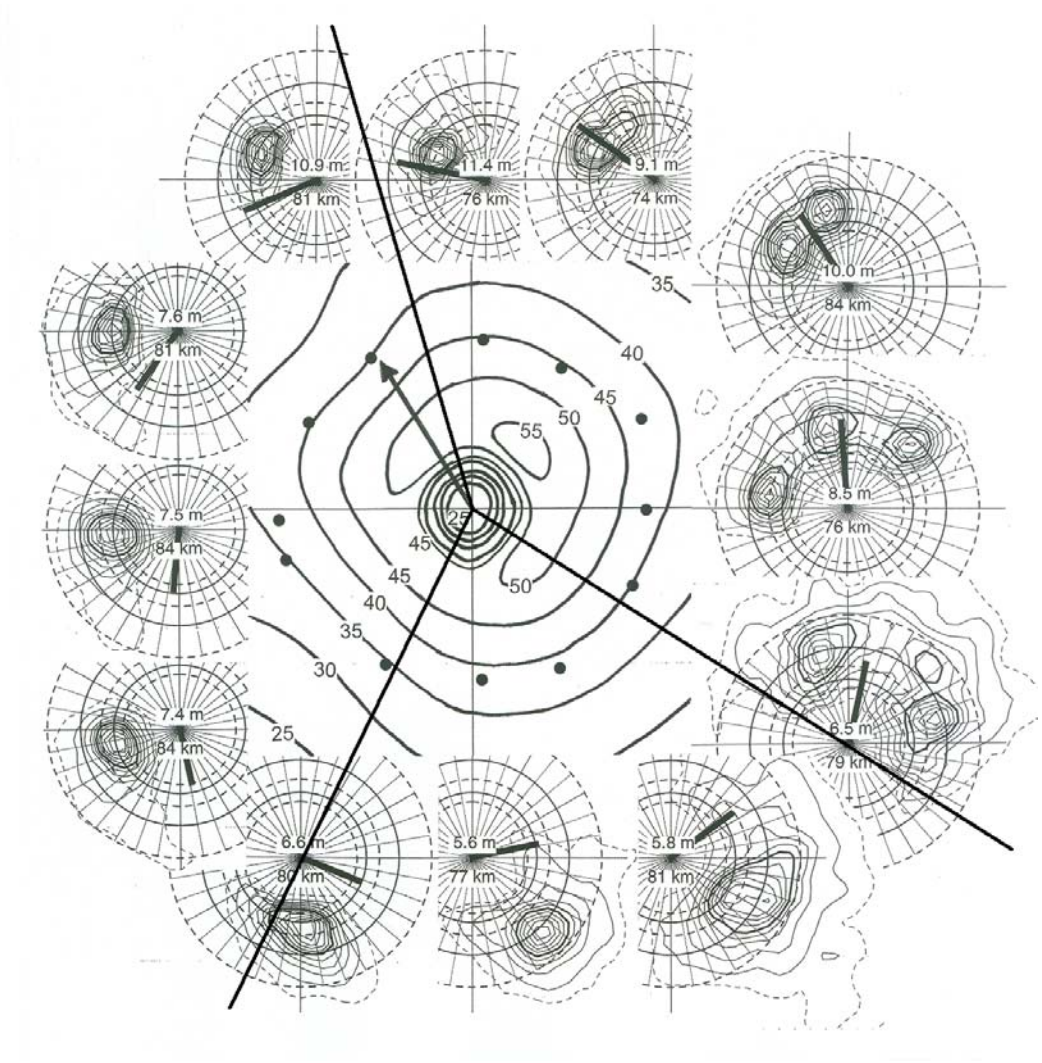

Figure 10. The center of the figure shows wind speed contours (ms-1) from the HRD H*WIND surface wind analysis- based mainly on SFMR surface wind speed measurements in Hurricane Ivan at 2230 UTC on 14 September 2004 for a 2° box in latitude and longitude centered on the eye. Arrow at the center indicates Ivan's direction of motion (330º). The storm-relative locations of twelve 2D surface wave spectra measured by the SRA are indicated by the black dots. The spectra have nine solid contours linearly spaced between the 10% and 90% levels relative to the peak spectral density. The dashed contour is at the 5% level. The outer solid circle indicates a 200 m wavelength and the inner circle indicates a 300 m wavelength. The dashed circles indicate wavelengths of 150, 250, and 350 m (outer to inner). The thick line at the center of each spectrum points in the downwind direction, with its length proportional to the surface speed. The upper number at the center of each spectrum is the significant wave height and the lower number is the distance from the center of the eye. The average radial distance for the twelve spectral locations is 80 km. The SRA data which produced the spectra were collected between 2030 UTC on 14 September and 0330 UTC on 15 September.

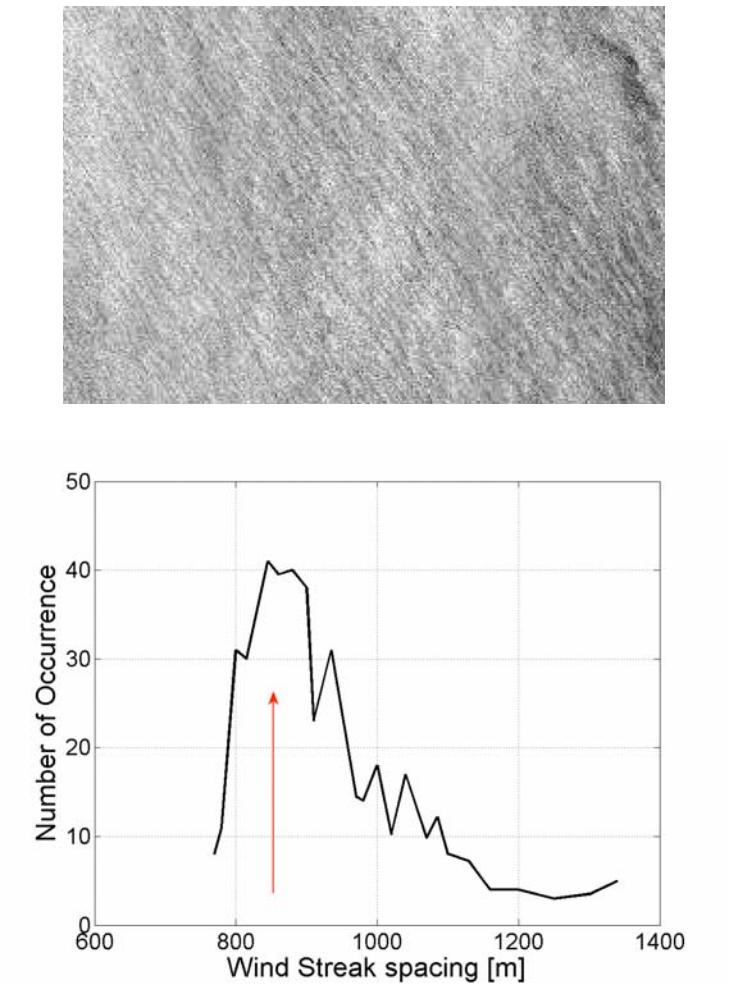

Figure 11. RADARSAT SAR image (top) from right-front quadrant of Hurricane Fran, similar to that obtained for Hurricane Isidore, 2002. The horizontal scale is 200 km. Histogram (bottom) of wind streak wavelengths from analyzed RADARSAT image of Hurricane Isidore, 23 September, 2002. Arrow indicates peak in aircraft-derived spectrum in Fig. 12. RADARSAT image courtesy of Canadian Space Agency.

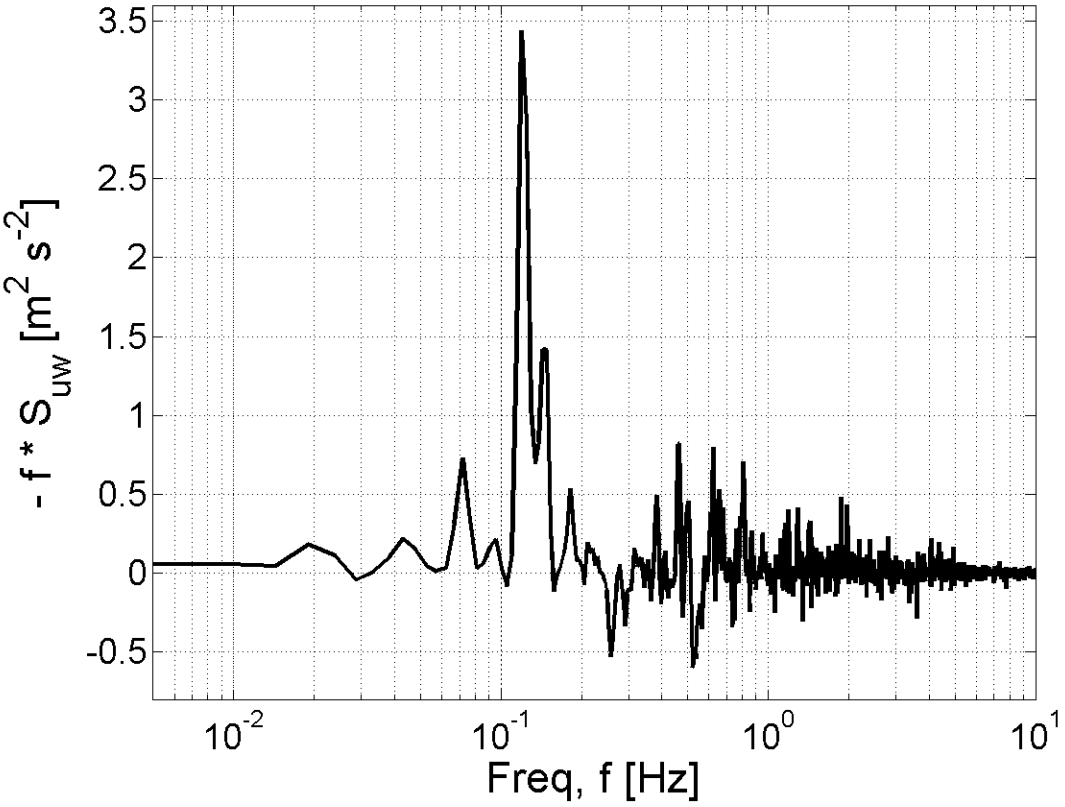

Figure 12. Co-spectrum of vertical momentum flux (-u'w') along a 120 m altitude radial flight leg into Hurricane Isidore, 22 September, 2002. The true air speed is 110 ms^{-1}.

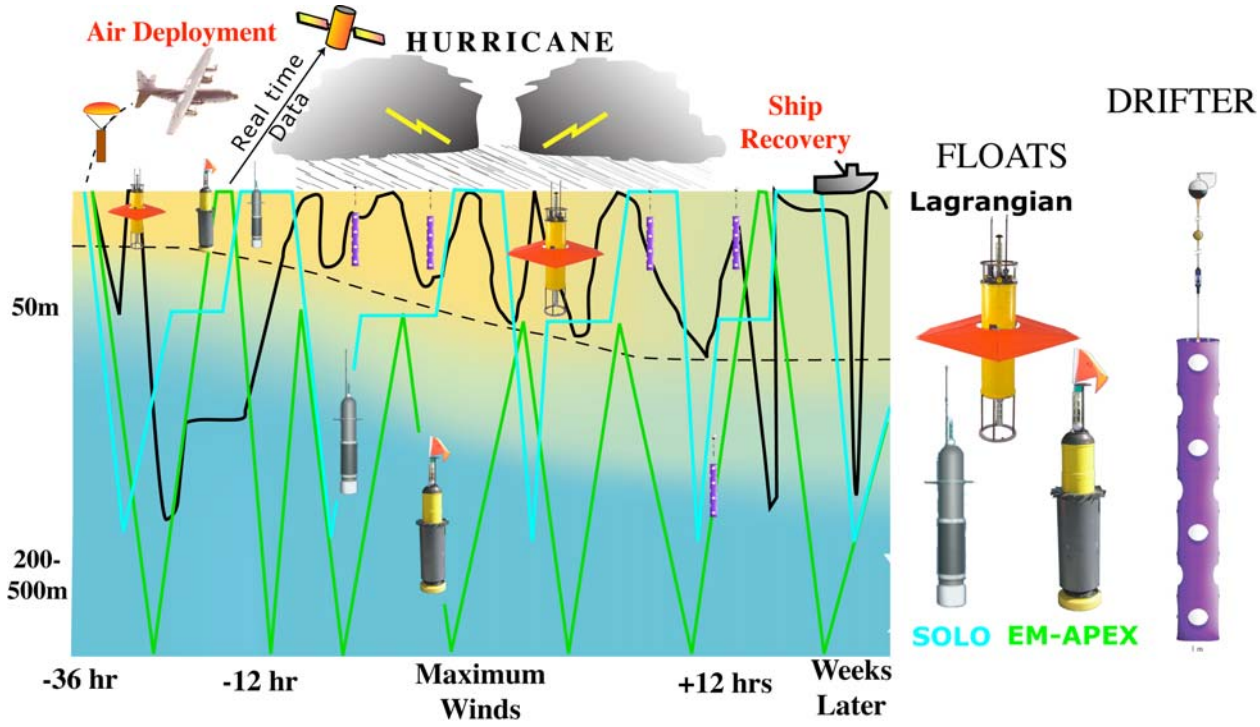

Figure 13. Drawings of the three varieties of floats and a surface drifter as deployed into Hurricane Frances. Schematic depicts operations in Hurricane Frances (2004).

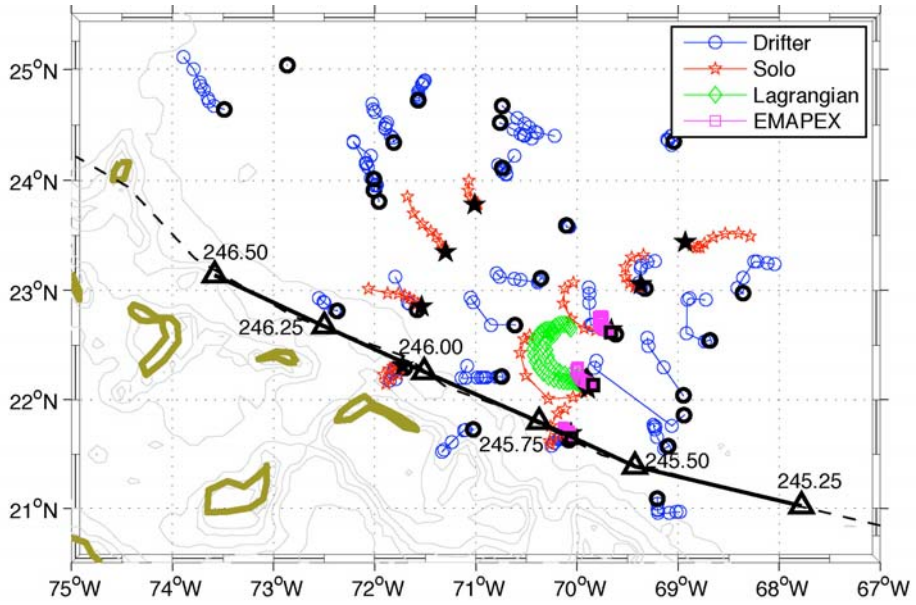

Figure 14. Hurricane Frances (2004) float and drifter array. Heavy line shows storm track, labeled by Julian Day (JD 245.00 = 1 Sept., 00 UTC). Colors indicate type of instrument. Instrument tracks are plotted from deployment on JD 244 (31 Aug) to JD 246.5 (2 Sept, 12 UTC). Deployment position is indicated by black symbol.

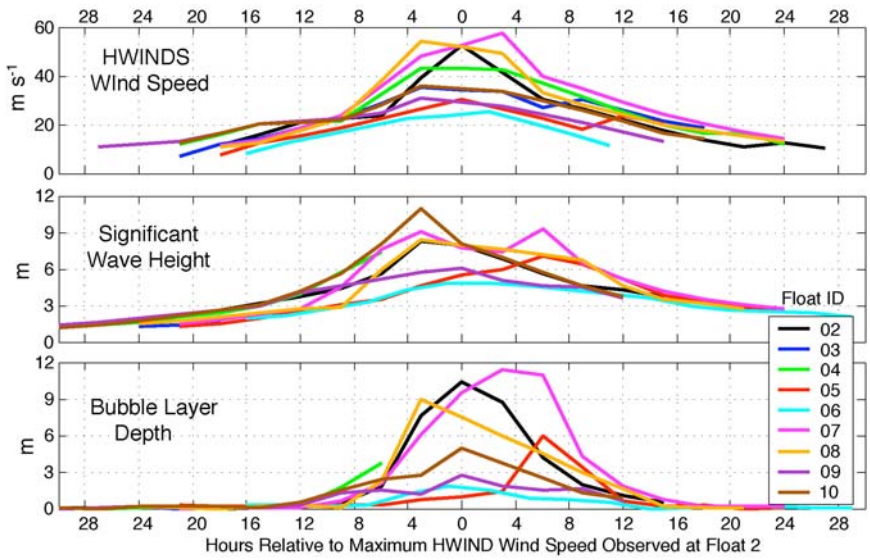

Figure 15. Significant surface wave height and bubble cloud depth measured by the 9 SOLO floats and wind speed at the float location from H*WIND analysis. Time axis is hours from time of maximum wind at each float.

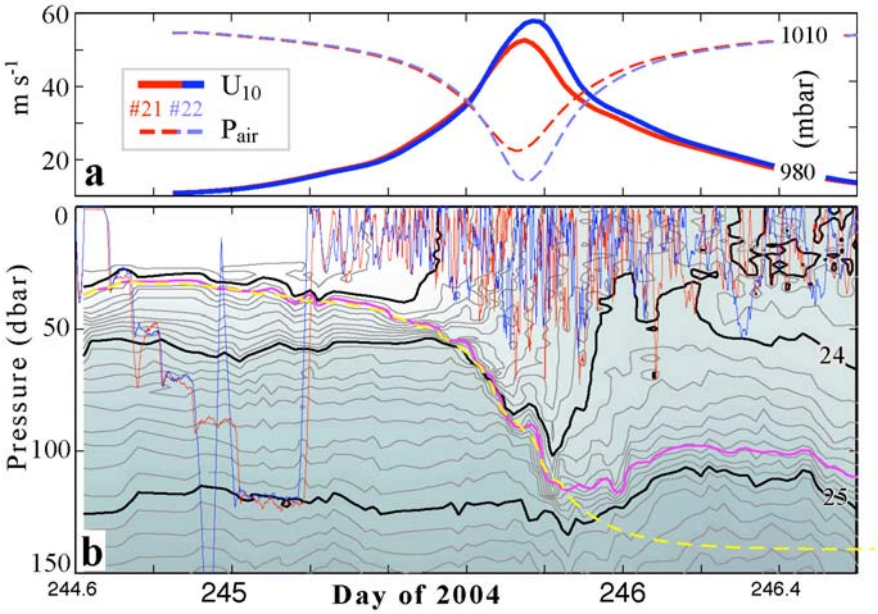

Figure 16. Evolution of the density structure of the upper ocean near the radius of maximum winds of Hurricane Frances. a) Wind speed and atmospheric pressure from HRD H*WIND analysis at the two Lagrangian floats. b) Potential density contours (kg m^{-3}) in black, trajectories of Lagrangian floats in red and blue, measured depth of the mixed layer in magenta and estimated depth of the mixed layer from a vertical heat budget in yellow (dashed).

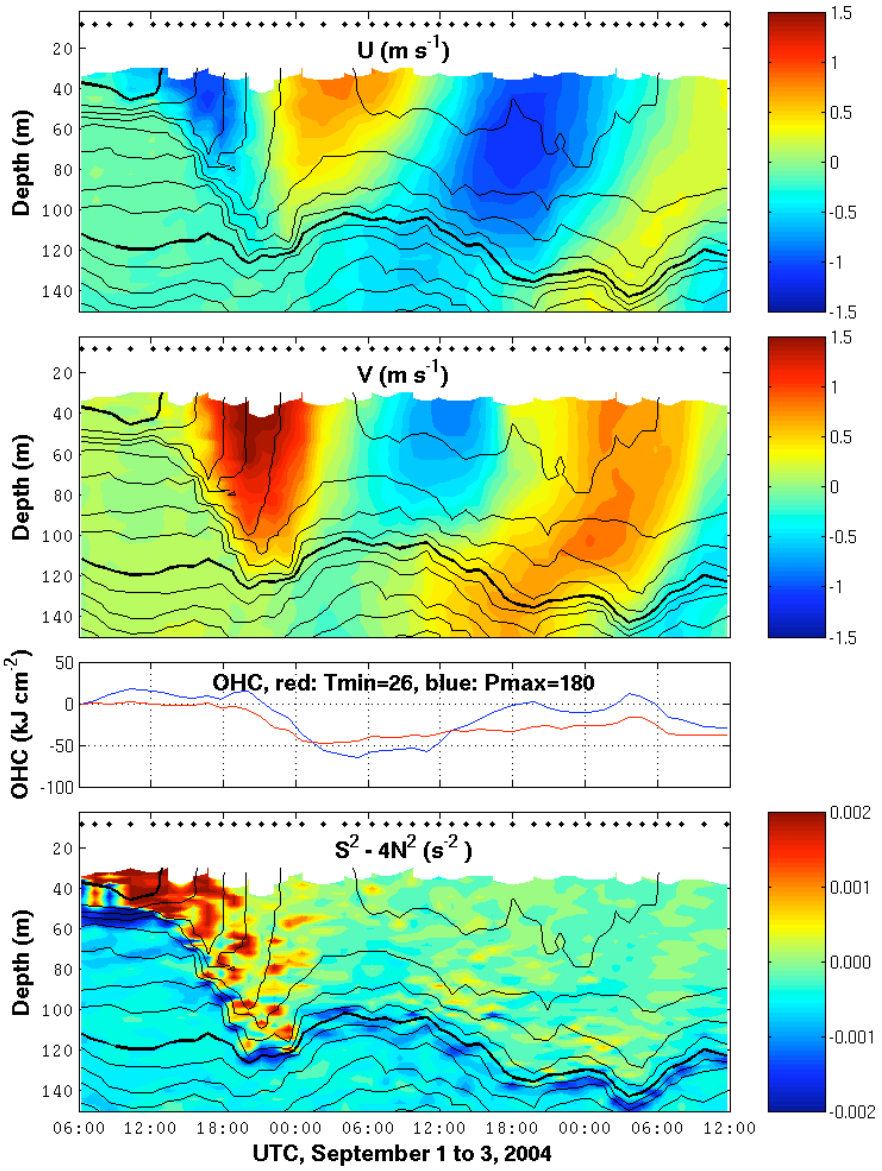

Figure 17. EM-APEX float 1633 located 50 km to the right of storm track in highest winds. The upper two panels are of East (U) and North (V) velocity components versus depth and time with the 29 and 25ºC isotherms in bold with a contour interval of 0.5ºC. The center of the storm passed at approximately 1700 UTC on Sept 1. Ocean Heat Content (OHC) is shown for water warmer than 26ºC and shallower than 180 m. The bottom panel is 'reduced shear', a stability parameter, with the temperature contours superimposed. This quantity is related to the Richardson number, $Ri=N^2/S^2$, where N is the Brunt-Väisälä frequency and S is the vertical current shear. A necessary condition for shear instability is $N^2/S^2 < 1/4$. This instability criteria is re-written as $S^2 - 4N^2 > 0$ to indicate where mixing is possible. The quantity $S^2 - 4N^2$ is contoured in the bottom panel with the green, yellow and red colors indicating where the instability criteria is equaled or exceeded. The blue colors indicate stable conditions less than zero.

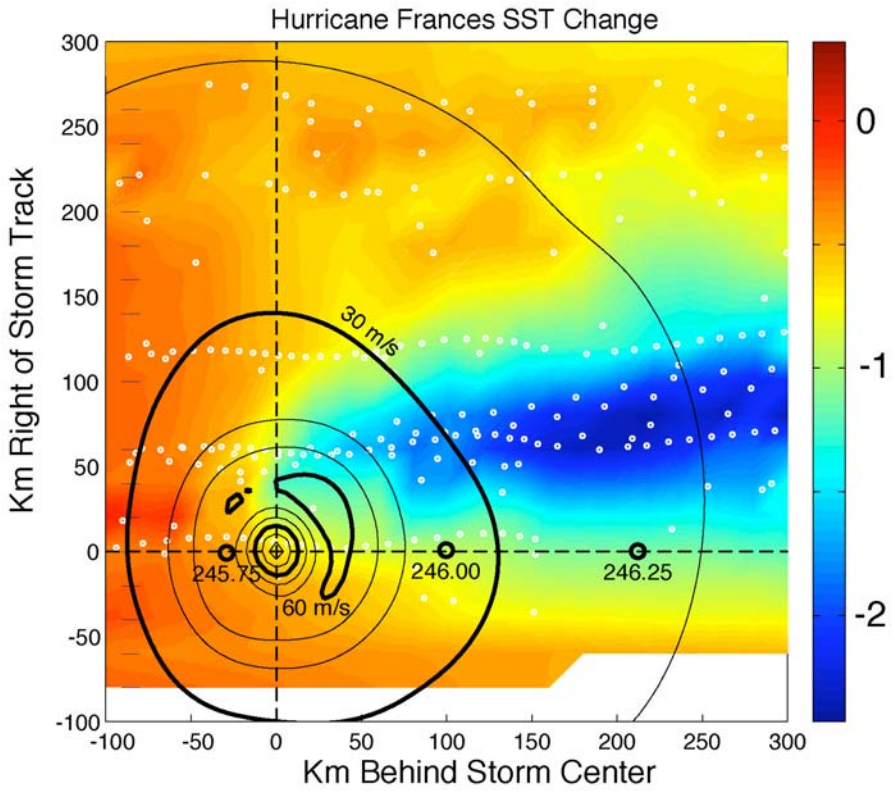

Figure 18. SST decreases (C) beneath hurricane Frances (2003) in storm-centered coordinate system. White dots show storm-relative locations of float and drifter data. Storm motion is to left. Colors show mapped SST change from pre-storm value. Contours show wind speed in ms^{-1} from H*WIND analysis. Storm positions are in increments of one-quarter Julian Days (JD), or 6 hours, where JD 245 is Sept 1.